Rare Met. (2022) 41(11):3591–3611
https://doi.org/10.1007/s12598-022-02061-7

RARE METALS

MINI REVIEW

Self-assembly of nanoparticles at solid–liquid interface for electrochemical capacitors

Xue Li, Chen Chen, Qian Niu, Nian-Wu Li*, Le Yu*, Bao Wang*

Received: 23 December 2021 / Revised: 19 February 2022 / Accepted: 8 March 2022 / Published online: 20 August 2022

Abstract Self-assembly of nanoparticles at solid–liquid interface could be promising to realize the assembled functions for various applications, such as rechargeable batteries, supercapacitors, and electrocatalysis. This review summarizes the self-assembly of the nanoparticles at solid–liquid interface according to the different driving forces of assembly, including hydrophilic–hydrophobic interactions, solvophobic and electrostatic interaction. To be specific, the self-assembly can be divided into the following two types: surfactant-assisted self-assembly and direct self-assembly of Janus particles (inorganic and amphiphilic copolymer-inorganic Janus nanoparticles). Using the emulsion stabilized by nanoparticles as the template, the self-assembly constructed by the interaction of the nanostructure unit (including metal, metal oxide, and semiconductor, etc.) not only possesses the characteristic of nanostructure unit, but also exhibits the excellent assembly performance in electrochemistry aspect. The application of these assemblies in the area of electrochemical capacitors is presented. Finally, the current research progress and perspectives toward the self-assembly of nanoparticles at stabilized solid–liquid interface are proposed.

Keywords Self-assembly; Solid–liquid interface; Driving force; Electrochemical capacitors

1 Introduction

Nanoparticles are small materials with one or more dimension, measuring in the nanometer scale range of 1–100 nm. In addition, nanoparticles have unique electronic, chemical and physical properties due to their high specific surface areas and nanoscale sizes, and many of their properties can be controlled by the degree of nanoparticles aggregation [1]. Self-assembly refers to the spontaneous assembly of building blocks into stable, well-defined new nanostructures, which plays an important role in the preparation of materials with special morphology [2, 3]. Superstructures of different or identical nanoparticles self-assembly in a particular way could realize multiple functions beyond the dispersed particles, which usually demonstrate novel properties in many applications, such as in superconducting materials, energy storage, electronic sensing [4]. As for the design and synthesis of nanomaterials, the assembling nanomaterials for ordered structures with various scales and structures, such as one-dimensional (1D) [5], two-dimensional (2D) [6, 7], or three-dimensional (3D) [8], resulting in novel coordinated characteristics. It is of great significance for the construction of micro-/nano-devices based on nanomaterials to realize the reasonable regulation in their microscopic size. For the application of devices, it is necessary to arrange these particles accurately to realize the specific functions.

Self-assembly of nanoparticles is a facile, cost-effective, operative method to prepare ordered functional

Xue Li and Chen Chen contributed equally to this work.

X. Li, B. Wang*
State Key Laboratory of Biochemical Engineering, Institute of Process Engineering, Chinese Academy of Sciences, Beijing 100190, China
e-mail: baowang@ipe.ac.cn

C. Chen, Q. Niu, N.-W. Li*, L. Yu*
State Key Lab of Organic-Inorganic Composites, Beijing University of Chemical Technology, Beijing 100029, China
e-mail: linianwu@mail.buct.edu.cn

L. Yu
e-mail: yule@mail.buct.edu.cn

superstructures [9, 10]. Functional materials with special electrical and other properties can be obtained by adjusting the distance and arrangement of nanoparticles [11, 12]. Nanoparticles can be used as basic building blocks to construct ordered structures from the nanometer or micron-scale by self-assembly technology. Superstructures with highly specific morphologies may generate new properties for applications in many fields [13, 14]. It is worth mentioning that interfacial self-assembly of nanoparticles is mainly carried out at liquid–liquid interface or liquid–gas interface.

Solid particles assembled in the Pickering emulsion could not reduce the interfacial energy directly. Therefore, the solid particles usually need outer force to minimize the surface energy for a thermodynamically stable state at liquid–liquid interface or liquid–gas interface [15, 16]. Solid particles irreversibly adsorbed at the oil/water interface or immersed in a continuous phase can provide steric hindrance between emulsion droplets to prevent the collision and coalescence [17]. When the colloidal particles move to the oil–water interface, the area of the oil/water interface would decrease and the interface energy of the system would decrease. At this point, the particles will be adsorbed at the interface. Emulsion stabilized by the solid particles can be used as a template to prepare organic/inorganic hybrid superstructure microcapsules and microspheres [18, 19] which are widely used in food, cosmetics, medicine, and other fields [20]. The driving forces of the self-assembly can be hydrogen bonds, van der Waals, magnetic forces, electrostatic forces, hydrophilic–hydrophobic interactions, surface organic molecular forces, and so on [21–23]. In this review, we summarize two typical superstructures assembled from the surfactants-assisted nanoparticles and Janus particles. The different driving forces in the assembly can be divided into hydrophilic–hydrophobic interactions, solvophobic and electrostatic interaction. In addition, the typical self-assembled superstructures at solid–liquid interface through different driving forces are highlighted (Fig. 1). The representative applications of self-assembled superstructures in the electrochemical capacitors, especially the aqueous hybrid supercapacitors (HSCs) and organic metal ion capacitors (MICs), are also briefly introduced. Finally, the development direction and challenges of the self-assembly of inorganic nanoparticles based on Pickering emulsion templates are prospected.

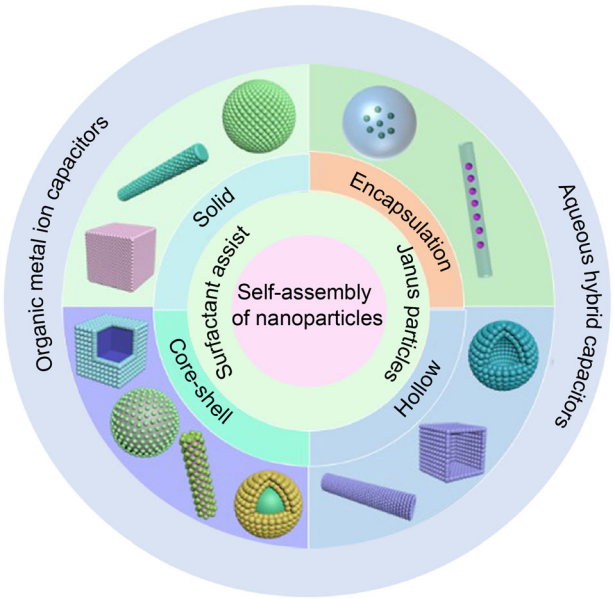

Fig. 1 Overview of self-assembly of nanoparticles at solid–liquid interface via different driving forces

2 Particle stabilized emulsions

The emulsion stabilized by solid particles is named Pickering emulsion [24, 25]. The type of Pickering emulsion is mainly determined by the wettability of the particles and can be characterized by the three-phase contact angles [26, 27]. When the solid particles are easily wetted by the water phase, i.e., $\theta < 90°$, it is easy to form oil-in-water (O/W) emulsion. On the contrary, when the solid particles are easily wetted by the oil phase, i.e., $\theta > 90°$, it tends to form water-in-oil (W/O) emulsion. However, when the particles are largely hydrophobic (large contact angle) or largely hydrophilic (small contact angle), they tend to remain in the oil or water phase, resulting in an unstable emulsion [28]. Theoretically, the adsorption of solid particles on the oil/water interface to form a stable emulsion requires a single hydrophilic or lipophobic surface, and the adsorption on the oil/water interface reduces the interface area and the surface energy. Therefore, the coalescence between emulsion droplets can be inhibited to ensure the formation of a durable and stable emulsion. The stability of solid particles in an emulsion is usually related to the desorption energy ΔE (the energy that excludes particles from the interface into the two-fluid phase). For a single smooth spherical particle of radius (R), assuming that the particle is in an ideal state, ΔE can be described in the following Eq. (1) [29]:

$$\Delta E = \pi R^2 \gamma_{o/w} (1 - \cos\theta)^2 \quad (1)$$

where $\gamma_{o/w}$ and θ represent the oil/water interfacial tension and the contact angle of particles at the oil/water interface, respectively. When R and $\gamma_{o/w}$ are constants, θ of particles at the interface of two phases is a very important variable parameter. According to Eq. (1), when $\theta = 90°$, ΔE value reaches the maximum, and at this time, the adsorption of colloidal particles at the oil/water interface is relatively

strong. Therefore, solid particles with the contact angle condition can form stable W/O emulsion or O/W emulsion, and the type of Pickering emulsion is mainly determined by the volume ratio of the oil and water phase. When the contact angle is larger than 160° or smaller than 20°, the ΔE decreases to 10 kBT or even smaller, which makes it difficult to form a stable emulsion. And then, the change of ΔE caused by the different wettability of particles is a key factor affecting the ability of particles to stabilize the emulsion. When particles are adsorbed to this interface, the interface free energy will decrease, and self-assembly of particles will occur under the driving of the principle of minimum interface free energy. Besides, the presence of particles at the interface causes the liquid–liquid interface to deform, resulting in capillary forces that bind the particles closer together.

Therefore, to obtain solid particles with moderate wettability and induce nanoparticle self-assembly, that is the formation of the amphipathic nanoparticles, it is usually necessary to modify the particle surface. The common modifiers are small-molecule surfactant, amphiphilic Janus particle (including inorganic Janus nanoparticles and amphiphilic copolymer-inorganic Janus nanoparticles). Figure 2 shows the two classical types of interfacial self-assemblies including the surfactants-assisted self-assembly and the self-assembly of Janus particles. The amphoteric surfactants can self-assemble at the interface of two different solvents to form micelles. As the surfactant can be absorbed on other particles, the attached particles can be assembled as a special morphology. Similarly, heterogeneous Janus particles could also distribute in the interface to generate secondary large particles. According to the type of surface modifiers, the self-assembly can be divided into surfactant-assisted and Janus particles. Surfactant molecules contain both hydrophilic head group and hydrophobic tail chain. Hydrophobic chains can gather the supramolecules together in polar solvents through hydrophobic interaction for the orderly assembly, because the head groups of ionic surfactants can interact with the functional molecules with opposite charges. Therefore, ionic surfactants are often chosen as one of the components for ion self-assembly. In addition, the hydrophobic chains are flexible and can bend freely, which promotes thermodynamic stability of the supramolecules during the process of

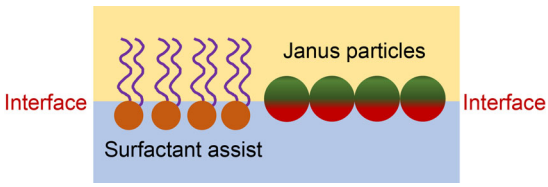

Fig. 2 Illustration of two classical types of interfacial self-assemblies of nanoparticles

assembly. Consequently, the ordered nanomaterials form mainly through hydrophobic interaction combined with ammonia bonding. Janus particles realize a unique asymmetry structure with different chemical or physical properties within a single particle, which offers an opportunity to access assembled structures [30]. When it "dissolves" in a good solvent of one block (but a poor solvent of the other), the poor solvent blocks would aggregate. Finally, the resulting micelle structure mainly includes a core formed by insoluble blocks and a flexible shell formed by soluble blocks. The structure of block polymer is precise, and its assembly shape can be effectively controlled by adjusting the molecular weight, different block lengths, and chemical composition. This method of encapsulating nanoparticles in micelles is based on the non-covalent interaction of solvophobic and electrostatic interaction between nanoparticles and block copolymers, which can be used to construct multifunctional capsules that show several desirable properties in a single micelle, thus broadening the range of applications [31]. The third section mainly lists the self-assembly of nanoparticles at solid–liquid interface, including the emulsions stabilized by nanoparticles modified with the small-molecule surfactants and Janus particles, according to the different driving forces of solvophobic and electrostatic interaction and hydrophilic–hydrophobic. The mechanism is briefly summarized; the advantages and development direction of each method are discussed.

3 Driving force of self-assembly of nanoparticle at solid–liquid interface

3.1 Surfactants-assisted self-assembly driven by hydrophilic–hydrophobic interactions

In many cases, solid particles often interact with surfactants or polymers to stabilize emulsions. The addition of surfactant or polymer has three functions as follows, which changes the wettability of the particle surface, promotes the flocculation of the particle, and reduces the oil/water interfacial tension. Binks and Murakami [27] studied the properties of emulsions cooperatively stabilized by SiO_2 and cetyltrimethylammonium bromide (CTAB). The addition of CTAB improves the contact angle of the particles and controlled the stability of the emulsion. No reverse of the emulsion was observed in the experiment. In addition, they also investigated emulsions stabilized by SiO_2 in conjunction with non-ionic surfactants [28]. The addition of surfactant leads to the decrease in flocculation and hydrophilicity of the particles, thus improving the stability of the emulsion stabilized by particles. The liquid crystal state of the surfactant with different shapes can be

obtained by adjusting the factors related to the liquid crystal state of the surfactant. The most important characteristic of the liquid crystal state is the directional arrangement of molecules, which can be used as a template for the formation of nanostructures. The concentration of the surfactant increases gradually due to the constant evaporation of the solvent, and the inorganic nanoparticles and organic molecules are distributed at both ends of the surfactant molecules, respectively, that is, the surfactant is used as a template for an orderly arrangement. When the surfactant concentration reaches the critical micelle concentration (CMC), the surfactant forms micelles. The corresponding inorganic and organic molecules are self-assembled by surfactant micelles induced by further volatilization of the solvent. Then, the meso-crystalline phase with a certain shape and periodic arrangement is formed, so that the inorganic and organic components can be assembled in a very short period into an orderly 3D regular sequence. Finally, the organic monomer or oligomer can be polymerized by light or heat, accompanied by the corresponding inorganic condensation process to maintain and fix the formed nano-organic sequence.

W/O, O/W, and oil-in-oil (O/O) emulsions are the ideal systems for the self-assembled superstructures. In these cases, the addition of surfactants to reduce surface tension can lead to the formation of tiny droplets, which are conducted in an interfacial driven W/O microemulsion process. Nanoparticle micelles self-assemble after evaporation of a drop of nanoparticle micelle aqueous solution. This interfacial process is driven by hydrophobic van der Waals interactions between the stabilizing ligand primary alkanes and the secondary alkanes of the surfactant, resulting in a thermodynamically defined cross bilayer structure [32]. In order to obtain stable emulsion, commonly used surfactants include poly sodium styrene sulfonate (PSS), polyethyleneimine (PEI), CTAB, sodium dodecyl sulfonate (SDS), polyacrylic acid (PAA), etc. Nanoparticles could assemble or aggregate on the surface between the two phases.

Some surfactants are used as templates for the assembly of inorganic nanoparticles. The absorption of surfactant on nanoparticles can reduce the surface energy of particles, control the morphology and size of the assembly and reduce the direct agglomeration of particles. Most of the atoms on the surface of the assembly would also produce new or enhanced properties of nanoparticles [33]. Dinsmore et al. [34] discovered that when an aqueous solution was added to an oil phase containing nanoparticles, an emulsion is formed in a few seconds by gently continuous shearing, which could be used as a template for nanoparticles to adsorb on the surface of the emulsion to reduce the total surface energy. These nanoparticles were either linked to polymeric cations, aggregated by van der Waals forces, or sintered together to form large particles. Surface adsorption caused colloidal microspheres in the suspension to pack closely on the shell of the emulsion droplets into spherical capsules with a single layer arrangement. The nanoparticles were transferred into water by centrifugation. Particles could be adsorbed and transferred to the oil emulsion in the outer layer of the water emulsion, which was attributed to the surface energy between the oil emulsion and the water emulsion was greater than that between the oil emulsion and the particles and the water emulsion and the particles.

Recently, it has been reported that hydrophobic Fe_3O_4, Au, SiO_2 and SdSe nanoparticles were assembled into 2D and 3D structures on the interface of chloroform-water. Using cyclohexane as the organic phase, Li et al. successfully self-assembled $BaCrO_4$, CdS, PbS, Fe_3O_4, ZrO_2, $NaYF_4$ nanoparticles, $PbSeO_3$ nanorods, Bi_2S_3, and LaF_3 nanoplates into 3D microsphere at the two-phase interface [35]. The preparation process is listed in Fig. 3a. Nanocrystals self-assemble into the colloidal particles driven by the van der Waals force. Colloid crystals are obtained by centrifugation and calcination to remove excess surfactants (Fig. 3b). The basic idea of this method is to use microemulsion droplets as a limiting template in which the nanoparticles assemble as the low-boiling solvent evaporates. Liu et al. [36] used Au nanoparticles as assembly units to assemble 3D plasma colloids (PCs) with hexagonal compact multilayer shells based on a novel 1-butanol aqueous reflectance emulsion system (Fig. 3c). The particle size of the obtained superstructure is relatively uniform (Fig. 3d, e). This is the result of strong coupling between plasma particles, which makes it have low reflectivity and strong wideband absorption. Zhao et al. [37] added polyvinylpyrrolidone to ethylene glycol to form microemulsion and prepared $ZnMn_2O_4$ hollow microspheres (Fig. 3f, g). Mn^{2+} and Zn^{2+} bond with polyvinyl pyrrolidone (PVP) to form spherical ZnMn-glycolic acid. With the evaporation of the solvent, 3D hollow $ZnMn_2O_4$ microspheres are obtained by the shrinkage and solidification of the ZnMn-glycolic acid microspheres.

Hyeon et al. have reported a study of the self-assembly of the magnetic nanoparticles using O/W emulsion as a template (Fig. 4) [38]. First, monodisperse nanoparticles with particle size of 11–12 nm were prepared by thermal decomposition method [39–41]. Then, mesoporous Fe_3O_4 nanoparticle clusters were prepared by bottom-up self-assembly method using dodecyltrimethylammonium bromide as a surfactant for emulsifying the oil–water interface. The addition of PVP polymers stabilized the nanoparticle clusters through spatial repulsive interactions and guided the nanoparticle clusters into a more ordered structure. A stable interface is achieved between the electrolyte and the active material by controlling the geometry,

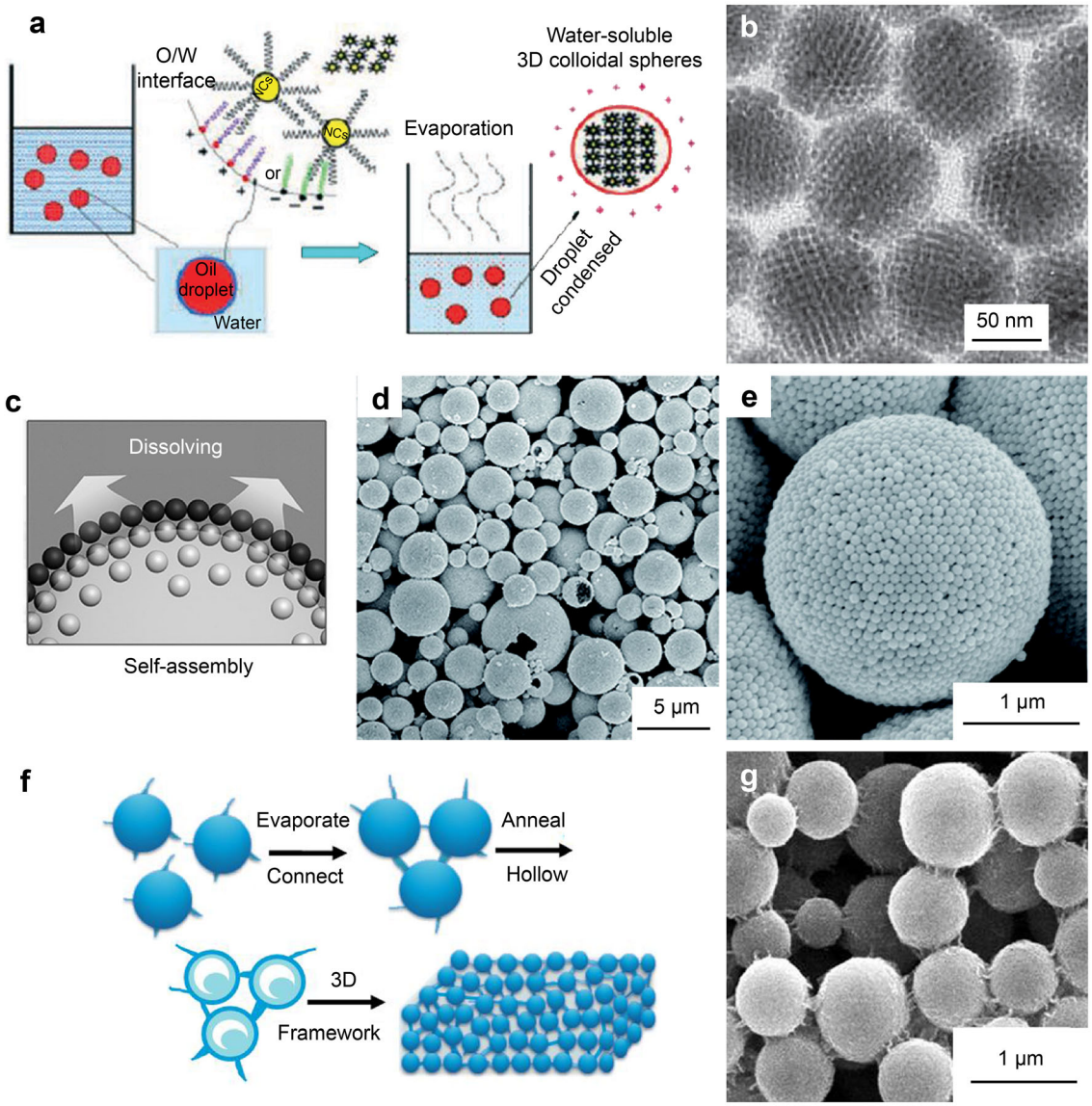

Fig. 3 Surfactants-assisted self-assembly of nanoparticles. **a** Schematic illustration of emulsion-based bottom-up self-assembly method; **b** high-resolution transmission electron microscope (HRTEM) image of $BaCrO_4$ colloids. Reproduced with permission from Ref. [35]. Copyright 2007, Wiley. **c** Self-assembled mechanism of multilayered plasmonic superstructures; **d, e** scanning electron microscope (SEM) images of self-assembled Au plasmonic superstructures. Reproduced with permission from Ref. [36]. Copyright 2015, Wiley. **f** Self-assembly process of hierarchical $ZnMn_2O_4$ hollow microspheres; **g** SEM image of self-supporting $ZnMn_2O_4$ microspheres. Reproduced with permission from Ref. [37]. Copyright 2014, Elsevier Publishing Group

which is beneficial to the improvement of the crushing and mechanical degradation due to volume expansion during the cycle. The assembly used as anode for lithium-ion batteries (LIBs) shows good cycle stability and rate performance.

This process allows surfactant-modified nanoparticles to assemble on the surface of oil droplets and induces the generation of new superstructures, which can be defined as water-dispersed colloidal particles composed of hundreds of nanoparticles. The formation of the assembled structure is mainly driven by the hydrophobic–hydrophobic interaction of the long alkyl chain during the slow evaporation of organic solvents. Various highly ordered assemblies can be prepared flexibly through weak interactions (such as electrostatic interaction, hydrogen bonding, van der Waals interaction). Recently, nanoparticle superstructures with a variety of components have been made using this principle. However, the assemblies created by this hydrophobic action are usually fragile. The hydrophobic–hydrophobic interaction between each nanoparticle is more easily broken compared with the covalent interaction, which limits the practical application of assemblies.

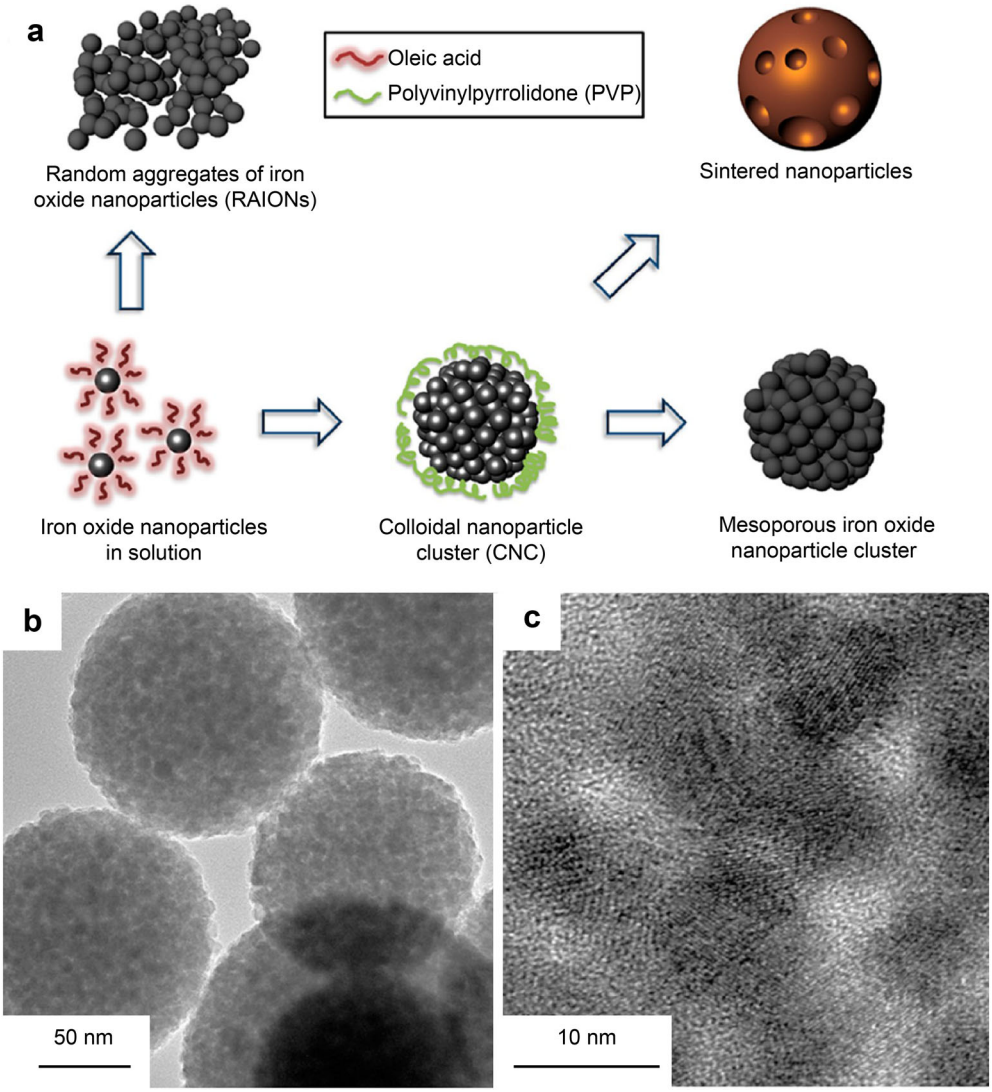

Fig. 4 Surfactants and auxiliaries-assisted self-assembly of nanoparticles: **a** schematic illustration of preparation of mesoporous iron oxide clusters and nanoparticles; **b, c** TEM images of mesoporous iron oxide superstructures. Reproduced with permission from Ref. [38]. Copyright 2013, American Chemical Society

Although the resulting assemblies possessed a uniform size and ordered nanoparticle arrays, disintegration of the superstructures could occur in long-term storage or under certain special conditions, such as violent agitation or the presence of organic solvents. Therefore, polymers are expected to improve the stability of the superstructures by forming core/shell superstructures, that is, the core of superstructures is bound to the polymer shell. For instance, PVP is used to form an assemblies/PVP superstructure. The chemical and physical stability of the superstructures is usually better than that of the original composite. However, the disintegration of the superstructures still occurs slowly due to the water-solubility of PVP. Superstructures decompose even faster after being stored in an alkaline solution for several weeks.

3.2 Self-assembly of Janus particles driven by solvophobic and electrostatic interaction

Janus particles not only possess the properties of emulsifier which can reduce the interfacial adsorption energy as solid particles, but also have the function of reducing interfacial tension due to the amphiphile properties similar to surfactant. Given this property, emulsions stabilized by Janus particles are more stable. In the Janus particle stable emulsion, the Janus structure parameter (JSP) (the ratio of the hydrophilic domain to the total particle volume) and the hydrophilicity of the Janus particle region are the key factors to determine the emulsion type. The amphiphilic Janus particles possess the properties of both colloidal particles and small molecular surfactants to stabilize

the Pickering emulsion, showing high desorption energy and the ability to reduce the surface tension. Consequently, Janus particles can form a stable emulsion.

3.2.1 Inorganic Janus nanoparticles

Inorganic Janus nanoparticles usually refer to metal oxide particles, such as SiO_2, Fe_3O_4, MnO, or TiO_2, which are partially covered by metal or inorganic nanoparticles or bimetallic Janus nanoparticles [42]. Chen et al. [43] created a Pickering emulsion stabilized an amphiphilicity of hydrogel-solid particles, the particles on the oil/water interface and without move even the vial is lean. The model of particles that stand at the interface and contact angle analysis was proposed to explain the reason. This emulsion not only possesses the kinetic stability of the Pickering emulsion prepared by isotropic particles, but also demonstrates the thermodynamic stability of the emulsion formed by using surfactant as an emulsifier. A variety of ordered aggregation structures, including bubbles, monolayer array structure, Pickering emulsion, crystal structure, and grid structure, can be obtained by orderly arrangement and assembly at the gas–liquid interface and liquid–liquid interface.

3.2.2 Amphiphilic copolymer-inorganic Janus nanoparticles

The mechanical properties of spherical aggregates induced by small-molecule compounds are very weak, which affects the subsequent application. The mechanical properties of self-assembled nanostructures induced macromolecular would be greatly improved. Polymer is a kind of typical soft material, which has a very sensitive response to a weak external field. Therefore, the ordered self-assembly of inorganic nanoparticles can be well guided by the appropriate design of organic polymers [44, 45]. Different from small molecular surfactants, polymer surfactants are used as both structural guide agents and organic components in the assembly, and the orderly assembled structure can be obtained without initiating polymerization. Polymers have high mechanical strength because of their long-chain segments and covalent bonds between chain segments. The structure of the superstructure cannot be destroyed under the condition of external stretching or compression. Nanoparticles would be distributed along the direction of external force, which is conducive to controlling the spatial distribution of nanoparticles in the polymer. The study of such hierarchically ordered organic–inorganic hybrid systems is of profound academic significance for understanding the synergistic effects of functionality and structure [46].

The compatibility between nanoparticle and block copolymer structure is an important factor to ensure the stable existence of nanoparticles in block copolymer substrate, which provides the possibility for nanoparticle self-assembly induced by block copolymer. One block in the block copolymer has attractive forces with the nanoparticle, such as chemical bonding, electrostatic force, and hydrogen bonding, while the other block has a repulsive action with the nanoparticles. The opposite force makes the nanoparticles stably exist in one end of the block copolymer, and various structures and patterns can be formed through the microphase separation of the two phases. Under certain conditions, the microphase separation of block copolymers can spontaneously self-assemble into regular structures with sizes ranging from several nanometers to dozens of nanometers. The phase separation of block copolymers in the nanoscale range provides a platform for the high dispersion of nanoparticles. Particles can be selectively implanted into the microphase of block copolymers by changing the interaction between nanoparticles and polymer, thus triggering the microphase separation of block copolymers. In principle, various forms of superstructures can be synthesized by implanting nanoparticles into micro-phases and controlling the dispersion and ordering of nanoparticles in the substrate material, which can be applied in various aspects.

3.2.3 Self-assembly of amphiphilic copolymer-inorganic Janus nanoparticles

Amphiphilic block copolymers are linear block copolymers. The general principle is described as a freezing-in of the middle block B by cross-linking (non-covalent) or covalent, while the incompatible blocks A and C point in different directions in the formed particle [47]. First, hydrophobic polymers are dissolved in organic solvents that are immiscible or slightly miscible with water. The solution is emulsified with water and an appropriate stabilizer to form a single or double emulsion. The solvent is then removed by evaporation or extraction into the excess continuous phase, converting the solvent droplets into solid particles or capsules. The assembly is generally spherical due to the interfacial tension between the aqueous and organic phases [48]. In addition, amphiphilic block copolymers can self-assemble into a variety of morphologies in selective solvents, including spherical, rod-like [49], lamellar [50], vesicles [51], large composite micelles and composite vesicles [52, 53].

When block copolymers are used as structural guides to induce self-assembly of nanoparticles (nanometals, metal oxides, semiconductors, etc.), high stability and size controllable self-assembled nanostructures can be obtained.

The research shows that the polymer with long flexible chains can improve the mobility of inorganic particles, reduce or eliminate the kinetic capture of inorganic particles and promote the thermodynamic equilibrium of the assembly system. Phase separation of block copolymers occurs in selective solvents to form micelles with core–shell structures. The self-assembly behavior of polystyrene-b-polyethylene glycol (PS-b-PEO) block copolymer in water was taken as an example. The hydrophilic part of the polyethylene glycol molecular chain unfolds in water due to solvation and plays the role of stabilizing micelles. However, the hydrophobic polystyrene chains tend to avoid contact with water and nucleate each other to reduce the interfacial free energy. After the shells of the self-assembled micelles are cross-linked, the hollow microspheres are obtained by removing the nuclei. At present, photoinitiation polymerization and cross-linking agent are generally used to cross-link the shell, and the core is removed by photodegradation or ozonation. Recently, many efforts have been devoted to the self-assembly of copolymer-induced particles, and various morphologies have been successfully assembled with magnetic nanoparticles [54], inorganic oxides [55], metal nanoparticles [56], and quantum dots [57]. Table 1 lists the morphology of nanoparticle self-assembly induced by amphiphilic copolymer [50, 54, 58–66].

Deng et al. [67] proposed a simple method for the direct synthesis of poly(4-vinyl pyridine) (P4VP)-based block copolymer Janus nanoparticles using solvent evaporation to induce nanoparticle self-assembly in emulsion droplets. Janus nanoparticle was formed due to the synergistic effect of solvent selectivity and interface selectivity, and the aspect ratio and Janus equilibrium could be fine-tuned. Janus nanoparticles could self-assemble into a multifunctional ordered superstructure (Fig. 5a, b). Yang et al. [68] used Fe_3O_4 and Au nanoparticles with a diameter of 6.5 and 3.5 nm as the structural units to create a "double Janus bilayer" on the liquid–liquid interface by using O/W microemulsion technology. The shell layer locked the nanoparticles with aliphatic ligand (oleic acid) at the liquid–liquid interface, and the nanoparticles were assembled into colloidal capsules in a regular arrangement. Besides, the method was also used to extend the growth to the lattice-mismatched binary nanocrystalline of Au/Fe_3O_4 $NaZn_{13}$ superlattice to achieve anisotropic superlattice growth and generate independent binary nanocrystals (Fig. 5c, d).

Iglesias et al. [69] described a reversible self-assembly method of nano-Au particles and theoretically demonstrated that the main driving force of Au nanoparticles self-assembly aggregation was hydrophobic action. The assembly process was accompanied by solvent evaporation (Fig. 5e). Finally, a core–shell complex with PS-b-PAA and PS-coated Au nanoparticles core was obtained, and thermal treatment of the quenched clusters makes them rigid and stable in aqueous solutions. (Fig. 5f). At present, many studies have been conducted on the self-assembly of nanoparticle induced by the amphiphilic block copolymer PS-b-PAA. Hickey et al. [59] reported the self-assembly of magnetic nanoparticles induced by PS-b-PAA molecules. Based on previous studies, the assemblers with three different morphologies were synthesized by adjusting the interaction between solvent types, nanoparticles and polymers, and the assembly mechanism was analyzed. For

Table 1 Nanoparticle self-assembly induced by amphiphilic copolymer

Particle type	Oil phase	Morphology	Assistant agent	Refs.
CdSe/ZnS	Dimethylformamide	Spherical	Poly(acrylic acid)-block-polystyrene (PAA-b-PS)	[58]
γ-Fe_2O_3	Dioxane	Encapsulation	PAA-b-PS	[59]
Fe_3O_4	Hexane	Solid spherical	Poly(2, 2, 3, 4, 4, 4-hexafluorobutyl methacrylate-graft)-poly(ethylene glycol) monomethacrylate) (HFMA-g-PEGMA)	[54]
Au	Chloroform	Helical	PS-b-P4VP(PDP)$_x$	[60]
PS-coated gold	Dimethylformamide	Chains	PAA-b-PS	[61]
Au	Chloroform	Solid spherical	Polystyrene-block-poly(2-vinylpyridine) (PS-b-P2VP)	[50]
Ag	Chloroform	Helical	PS-b-P4VP	[62]
CdSe	Chloroform	Lamellar	PS-b-P4VP	[63]
Au	Dichloromethane	Lamellar	PS-b-P2VP	[64]
Au-OH	Dimethylformamide	Cylinders	PS-b-PEO	[65]
Fe_3O_4	Toluene	Hollow spherical	Polyisoprene-block-poly(ethylene oxide) (PI-PEO)	[66]

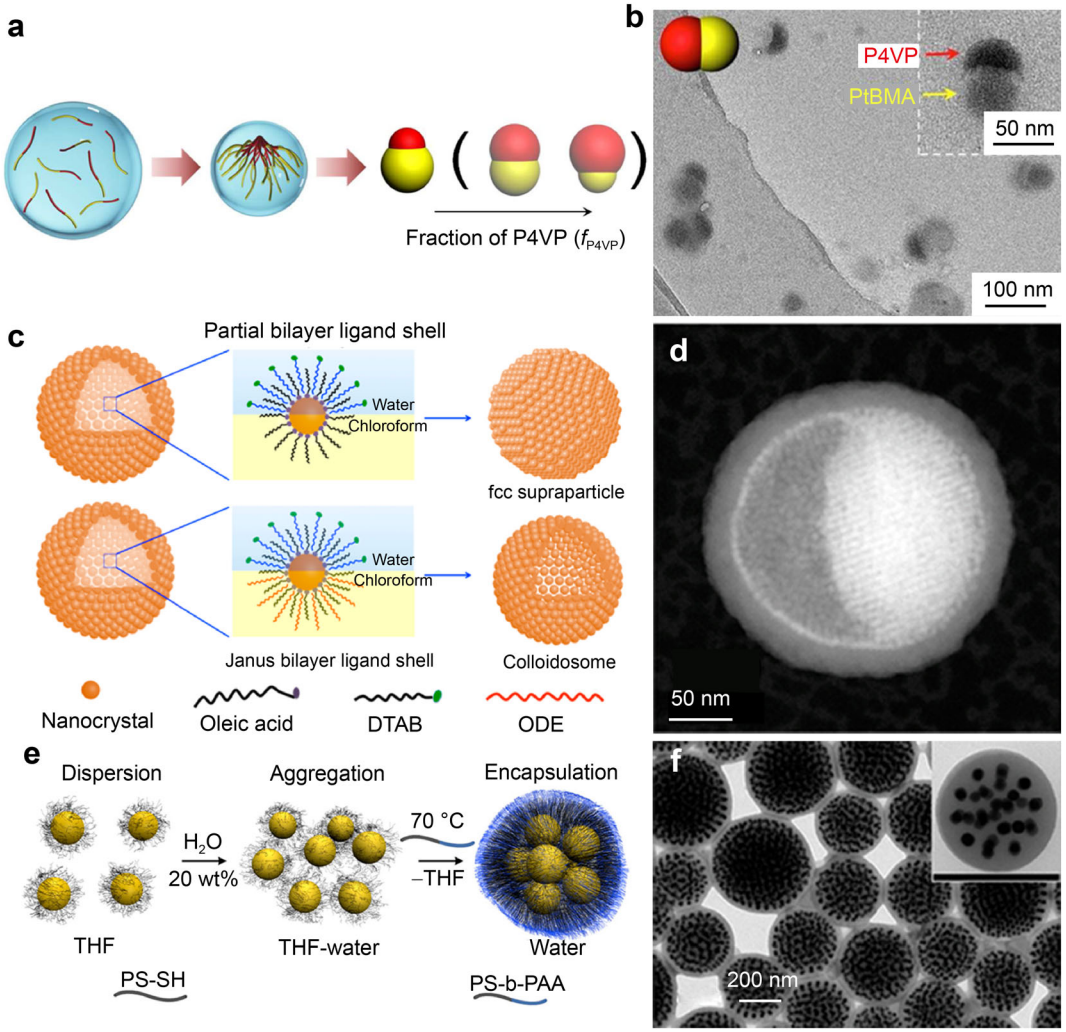

Fig. 5 Self-assembly of amphiphilic copolymer-inorganic Janus nanoparticles. **a** Illustrative synthesis of Janus nanoparticles by solvent evaporation induced assembly of P4VP-based di-block copolymers in emulsion droplets; **b** TEM image of Janus nanoparticles and crescent nanoparticles. Reproduced with permission Ref. [67]. Copyright 2016, American Chemical Society. **c** Schematic illustration of formation mechanism of nanoscale colloidosomes: a key step is to form Janus bilayer on nanocrystal surfaces, where DTAB is dodecyltrimethylammonium bromide, ODE is octadecene; **d** 2D HAADF-STEM projection image from tilt series of half-filled superstructures. Reproduced with permission from Ref. [68]. Copyright 2016, American Chemical Society. **e** 3D self-assembly of Au@PS nanoparticles, where THF is tetrahydrofuran; **f** TEM image of Au@PS nanoparticles. Reproduced with permission from Ref. [69]. Copyright 2012, American Chemical Society

example, when the solvent was tetrahydrofuran, the large micelles composites were formed. When N,N-dimethylformamide (DMF) was used as a solvent, the polymer formed spherical micelles. By adjusting the ratio between DMF and tetrahydrofuran, aggregates with different morphologies could be obtained, such as vesicles, spheres, and rod-like micelles. The effects of nanoparticles on the self-assembled structure of amphiphilic block copolymers and nanoparticles were investigated. They showed how the arrangement of nanoparticles in a polymer matrix could be controlled by manipulating solvent–nanoparticle and polymer–nanoparticle interactions.

On the other hand, there are many examples of hydrophobic alkyl-capped nanocrystals synthesized by pyrolytic metal precursors encapsulated by other amphiphilic block copolymers, such as polyisoprene-block-poly(ethylene oxide) (PI-b-PEO), PS-b-P4VP (PDP), and polybutadiene-block-poly(ethylene oxide) (PB-b-PEO) [66]. Zhu and Hayward [70] reported that iron oxide nanoparticles were embedded in worm-like micelle nuclei through the interfacial instability of emulsion droplets containing the amphiphile polymer PS-b-P4VP (PDP). However, it is difficult to achieve high loading and uniform dispersion of nanoparticles in the worm-like micelle core.

Accurate control of the location and uniform distribution of nanoparticles in the worm-like micelle core remains a challenge. Subsequently, they introduced a simple and general approach to solving this problem by embedding nanoparticles in micellar nuclei through the direct supramolecular assembly [71, 72]. The micelle morphology and the distance between nanoparticles could be adjusted by changing the concentration of nanoparticles and the PDP blocks. Sanwaria et al. [62] studied the control and localization of nanoparticles in the microphase separation structure of block copolymers from both theoretical and experimental aspects. The helical stacking of nanoparticles in the cylindrical of block copolymers was reported for the first time.

3.3 Distribution and localization of nanoparticles in block copolymers

Block copolymers can induce nanoparticles to form ordered, thermodynamically stable hybrid aggregates and regulate the morphology and distribution of nanoparticles in the assembly. The driving force lies in the equilibrium between the conformational entropy of the block copolymer, the conversion entropy of the nanoparticles, and the enthalpy of the interface between the nanoparticles and the block copolymer in the hybrid system. The conversion entropy of nanoparticles and the conformational entropy of polymers mainly depend on the size of nanoparticles and the mean square rotation radius (R_g) of block copolymers, and the interfacial free energy depends on the compatibility between the nanoparticles and block copolymers. The synergistic self-assembly of macromolecules and nanoparticles can effectively regulate the distribution of nanoparticles and form special self-assembly structures, such as hollow structures and double-layer spherical structures. Sánchez-Iglesias et al. [73] controlled the number and distribution of nanoparticles in the hybrid self-assembly. A layer of permeable SiO_2 nano-capsules was coated on the surface of the self-assembly of Au nanoparticles with a fixed number, which not only strengthened the assembly, but also improved the hydrophilicity and biological activity of the material. The size, concentration, and surface chemical modification of nanoparticles are the main factors affecting the distribution and localization of nanoparticles in block copolymer micelles.

3.3.1 Size of nanoparticles

The size of nanoparticles plays an important role in controlling the distribution and localization of nanoparticles in block copolymers. The hybrid assembly process of nanoparticles and block copolymers is mainly controlled by the total free energy in the system. When the particle size of nanoparticles is much larger than the mean square (R_g) of the polymer, the thermodynamically stable nanocomposite hybrid assembly cannot be formed. When the radius of the nanoparticle is basically equal to the polymer R_g, the conformational entropy loss by the polymer increases, and the translational entropy gained by the nanoparticle decreases. At this point, the nanoparticles are selectively distributed in specific microregions of the polymer. When the size of the nanoparticles is smaller than the R_g of the polymer segment, the system is mainly controlled by the translational entropy of the nanoparticles, the nanoparticles can be uniformly distributed in the micelles of the block copolymers.

3.3.2 Surface properties of nanoparticles

The compatibility of block copolymers with nanoparticles is an important factor in forming thermodynamically stable hybrid aggregates. The attraction between nanoparticles and block copolymers can be improved effectively by modifying the surface of nanoparticles with small molecules or short-chain polymers that are compatible with block copolymers, which can control the distribution and localization of nanoparticles in the block copolymer matrix. Park et al. studied the effects of different ligands on the distribution and localization of gold nanoparticles in micelles [74], using 1-undecanethiol and 1-dodecanthanol as ligands to stabilize gold nanoparticles, and assembled them with two block copolymer PS-b-PAA. When modified with two ligands, nanoparticles were distributed on the PAA and PS interfaces of spherical or rod-like micelles. When modified with a single ligand, 1-dodecanthanol molecule, the nanoparticles were concentrated in the nuclei of the spherical micelles (Fig. 6a).

3.3.3 Shape of nanoparticles

The shape of nanoparticles can also affect their arrangement and distribution in the hybrid assembly. Li et al. [75] explored the self-assembly behavior of gold nanorods and block copolymers. Two types of polymers with different segment lengths were used to modify the gold nanorods to control the arrangement of the nanorods in the micelles. It was found that the nanorods could be arranged in a "head-to-head" or "side-by-side" in the cylinder micelles (Fig. 6b, c). He et al. simulated the self-assembly of diblock copolymer-induced nanorods using dissipative particle dynamics method [76]. The results showed that the addition of nanorods can change the morphology of macromolecules. With the increase of the length of nanorods, the structure of the assembly would successively change from layered to lamellar and cylinder, band-like, cylinder, as shown in Fig. 6d. At the same time, the change

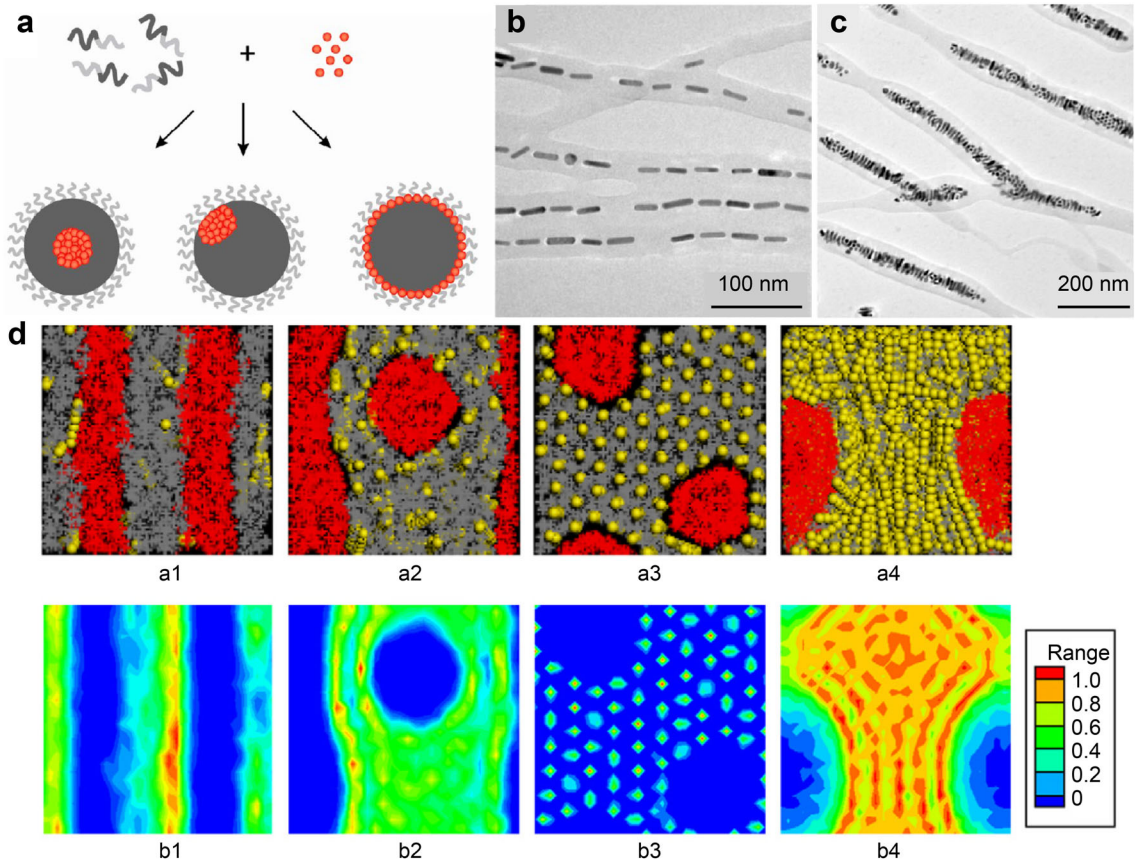

Fig. 6 Distribution of nanoparticles in block copolymers. **a** Pictorial description of self-assembly of PS_{250}-b-PAA_{14} and Au nanoparticles with varying surface ligands. Reproduced with permission from Ref. [74]. Copyright 2013, American Chemical Society. Bright-field TEM images of hybrid micelles formed from: **b** PS_{51k}-b-$P4VP_{17k}(PDP)_{2.0}$; **c** PS_{110k}-b-$P4VP_{107k}(PDP)_{1.0}$ encapsulated of nanorods (content of 27 vol%, diameter of 7 nm, and length of 29 nm), where nanorods were grafted with mixed PS brushes (PS_{2k}:PS_{12k} = 1:1). Reproduced with permission from Ref. [75]. Copyright 2013, American Chemical Society. **d** Morphologies and nanorod concentrations. Reproduced with permission from Ref. [76]. Copyright 2010, Elsevier

of the self-assembled structure would lead to the significant change of its mechanical properties.

The abundant physical and chemical properties of block macromolecules will provide a great development space for the hierarchical and ordered self-assembly of inorganic nanoparticles. The addition of block copolymer can not only induce the self-assembly of inorganic nanoparticles into various structures, but also effectively enhance the structural stability of the assembly. Understanding the basic principles of the hybrid assembly of copolymers and nanoparticles can lay a theoretical foundation for the design and preparation of superstructures with special mechanical and electric properties.

4 Applications of self-assembled superstructures for electrochemical capacitors

The increasing energy demands have provoked intense research for the advanced electrochemical energy storage systems. Electrochemical capacitors serve as an important category of energy technologies, which are receiving more attention than ever before [77, 78]. Using the emulsion stabilized by nanoparticles as the template, the self-assembly constructed by the interaction of the nanostructure unit (including metal, metal oxide, and semiconductor, etc.) not only possesses the characteristic of nanostructure unit, but also exhibits the excellent assembly performance in electrochemistry aspect. To be specific, as for the supercapacitors, cycling stability of the electrode is also an important evaluation criterion for supercapacitors. The self-assembly of nanoparticles leads to the formation of thermodynamically stable structures, which is beneficial to enhance the cycling performance of supercapacitors. Besides, the side reactions can be effectively restrained due to the reduced surface area. In some special cases of multilayered or multi-shelled structures, the mass transfer could be further promoted. Therefore, it shows great potential in the applications of HSCs and MICs.

4.1 Self-assembled superstructures for HSCs

The unique electronic, chemical and physical properties of nanomaterials extremely accelerate the development of energy materials, and the introduction of self-assembly technology of nanomaterials also greatly improves and enriches various properties of advanced energy materials. HSCs can bridge the gap between high-power density and high-energy density of capacitors and batteries [79–85]. In the last few years, the self-assembly and performance development of oxide nanomaterials have been studied extensively. Li et al. [86] reported a novel sodium-ion capacitor with a peanut shell structure by self-assembling Nb_2O_5 nanosheets. The capacitor presented a stable cycling, and its power density and energy density reached 5760 $W{\cdot}kg^{-1}$ and 43.2 $Wh{\cdot}kg^{-1}$, respectively. Huang et al. [87] have reported a facile synthesis of transition metal oxide-based hollow materials for HSCs. The Co_3O_4 hollow supraparticles embedded in the carbon nanofiber (CNF/HSP-Co_3O_4) and reduced graphene oxide (RGO/HSP-Co_3O_4) were generated schematically (Fig. 7a). TEM image (Fig. 7b) clearly elucidates the heterogenous hollow structure of CNF/HSP-Co_3O_4. HRTEM image reveals that the bubble-like Co_3O_4 hollow spheres were attached on the exterior of CNF with the assistance of a ultrathin carbonaceous layer (Fig. 7c, d). Electrochemical impedance

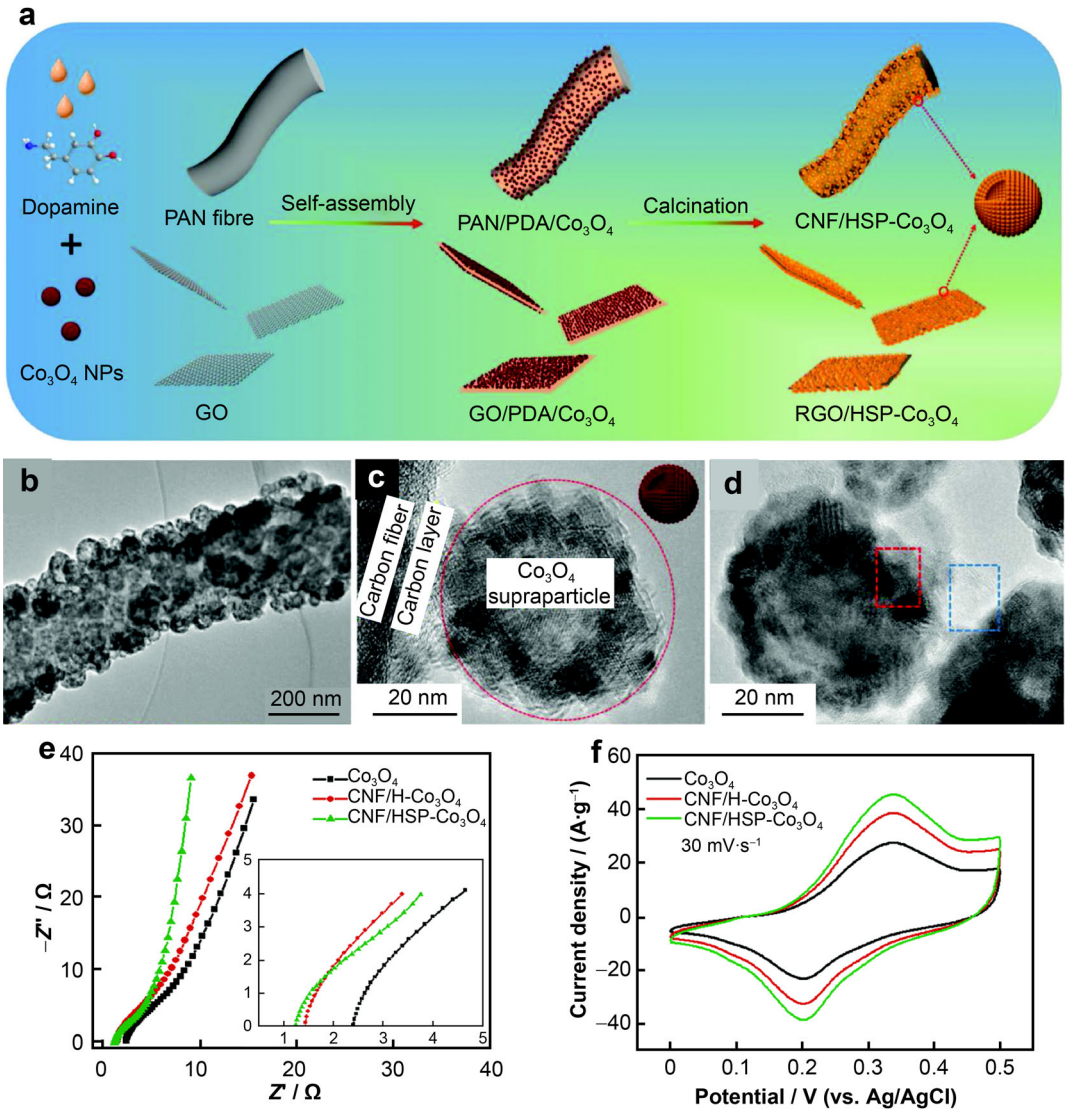

Fig. 7 **a** Schematic illustration of fabrication of CNF/HSP-Co_3O_4 and RGO/HSP-Co_3O_4, where PAN is polyacrylonitrile; **b** TEM image of an individual fiber of CNF/HSP-Co_3O_4; **c** HRTEM image of enlarged interface between CNF and Co_3O_4 supraparticles and (inset) schematic illustration of an individual supraparticle; **d** HRTEM image of enlarged interface between Co_3O_4 supraparticles; **e** Nyquist plots (Z', real part of impedance; Z'', imaginary part of impedance) and **f** CV curves of Co_3O_4, CNF/H-Co_3O_4 and CNF/HSP-Co_3O_4 at a scan rate of 30 $mV{\cdot}s^{-1}$. Reproduced with permission from Ref. [87]. Copyright 2019, Wiley

spectroscopy (EIS) was employed to study the electrons/ions conductivity of the different HSC anodes. The corresponding EIS data (Fig. 7e) show that the series resistance (R_s) of the Co_3O_4 electrode was greatly reduced by the conductive CNF matrix. The cyclic voltammetry (CV) curves in Fig. 7f show that the CNF/HSP-Co_3O_4 electrodes testify substantially larger capacitance at a scan rate of 30 mV·s^{-1}. Benefitting from the self-assembly of ultrafine Co_3O_4 nanoparticles with the help of polydopamine (PDA) and the unique hybrid architecture, the heterogenous hollow electrodes present an enhanced utilization ratio of active materials and high ionic/electronic conductivity.

With regard to various structural and compositional features, metal–organic frameworks (MOFs) produced by the assembly of metal ions with organic ligands are utilized as a novel type of reactants to build hollow materials [88–95]. It is worth mentioning that hollow MOFs facilitate the formation of complex hollow structures constructed from diverse primary subunits [96–99]. Guan and Lou [100] exploited a "nanoparticles-in-MOF" self-templated method for the synthesis of complicated bubble-like CoS nanocages, which is schematically depicted in Fig. 8a. TEM image shown in Fig. 8b presents the hollow structure of the complex CoS nanocages. A enlarged view indicates that the CoS nanocage is constructed from numerous ultrafine highly dispersed nanobubbles (Fig. 8c, d). Besides, this "nanoparticles-in-MOF" self-templated approach can be applied to put different functional species including Zr-MOF nanoparticles, rod-like FeOOH, or carbon nanotubes (CNTs) in ZIF-67 during its growth. Owing to the special shell structure and stable support, the derived bubble-like CoS nanocages show enhanced electrochemical activity as anode for HSCs. Figure 8e presents typical CV curves of bubble-like CoS nanocages and the normal CoS cages, which proves that bubble-like structure could store more charges due to the structural superiority. The rate performance of different electrodes is shown in Fig. 8f. To be specific, the bubble-like CoS nanocages present a large specific capacitance of 1060 F·g^{-1} at the current of 1.0 A·g^{-1}. Even at a rather high current of 20 A·g^{-1}, a high capacitance of 764 F·g^{-1} can still be maintained.

Other than the self-assembly processes driven by van der Waals and hydrogen bond, electrostatic self-assembly is also a novel strategy to assemble diverse functional nanoparticles with opposite charges through electrostatic interaction. Therefore, it requires an additional surface functionalization process for the subsequent formation of the uniform complexes [101–105]. For example, MXenes can be negatively charged by the surface functional groups during the synthesis, which lays an excellent foundation for the electrostatic self-assembly [106]. Similarly, Xie et al. [102] demonstrated a $Ti_3C_2T_x$/CNT composite assembled by the negatively charged MXene nanosheets and CTAB modified CNTs with positively charges. Wu et al. [107] proposed 2D interstratification assembly for the hybrid electrodes of MXene/NiCo-LDHs from the CTAB modified MXene nanosheets (MXene-CTAB) and sodium dodecyl benzene sulfonate (SDBS) modified NiCo-LDHs (NiCo-LDHs-SDBS) for electrochemical capacitors. Figure 9a illustrates the fabrication of the MXene/NiCo-LDHs electrode through electrostatic adsorption of interlayer cations and anions. The assembly of alternating single layers of MXene and NiCo-LDHs with an interstratification spacing of 1.5 nm could alleviate the self-restacking of each 2D materials (Fig. 9b, c). The MXene/NiCo-LDHs composite electrodes also have outstanding electrochemical property thanks to its unique structural characteristics. When the current density increases from 2 to 20 mV·s^{-1}, the shape of CV curves of MXene/NiCo-LDHs electrodes retains the same. Although the anodic–cathodic peaks shift slightly, there is no apparent deformation, indicating good rate capacitance and Faradaic redox reaction (Fig. 9d). From Fig. 9e, all the galvanostatic charge–discharge curves demonstrate good symmetries at the current densities from 0.5 to 10.0 A·g^{-1}, which prove that the MXene/NiCo-LDHs electrodes have high Coulombic efficiency in the charge–discharge processes.

4.2 Self-assembled superstructures for lithium-ion capacitors (LICs)

The self-assembly from nanoparticles to micron particles obtains multi-level structure, specific size and morphology, showing better various properties and alleviating the agglomeration and pulverization of particles that may occur in the process of charging and discharging cycles of simple low-dimensional nanomaterials, which may affect their electrochemical performance. LICs have attracted great attention because of their high energy/power densities, which bridges the gap between batteries and electrochemical capacitors [108–112]. The key to high-performance LICs is to find appropriate electrode materials to overcome the dynamic imbalance between the sluggish Faradic reaction of the battery anode and fast non-diffusion-controlled process of the capacitive cathode (Fig. 10a). Hu et al. [113] reported an innovative self-assembly strategy for the synthesis of homogeneous binary organic particles as anode materials with fast lithium absorption mechanisms for the fabrication of high-energy LICs with high flexibility. Maleic acid (MA) and polyvinylidene fluoride (PVDF) are co-dissolved into N-methylpyrrolidone (NMP), resulting in a uniform mixture of both at the molecular level. By solvent evaporation, the dissolved MA and PVDF molecules are coprecipitated and self-assembled as MA@PVDF binary organic particles

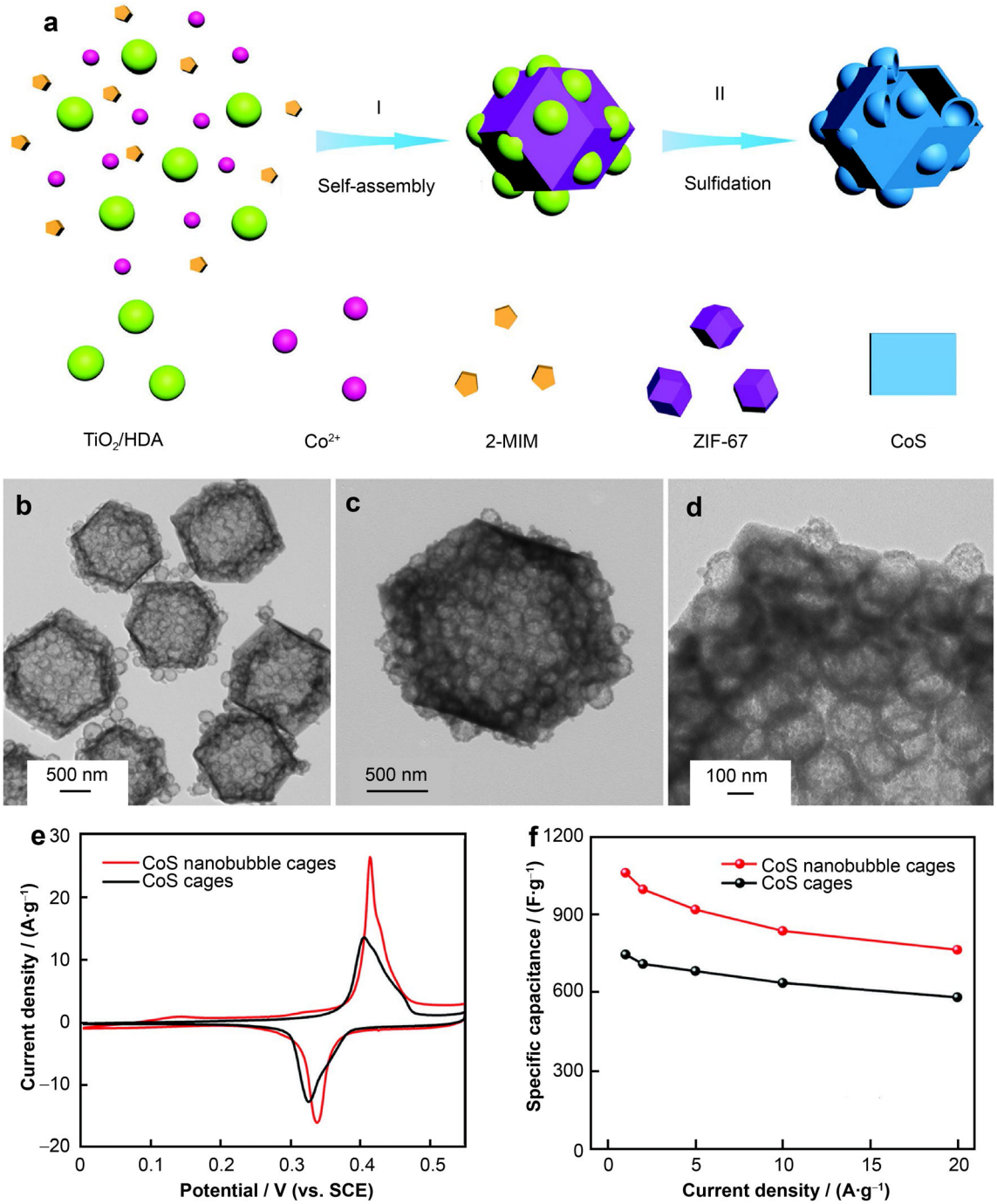

Fig. 8 **a** Schematic illustration of controlled encapsulation and conversion processes for bubble-like CoS nanocages, where 2-MIM is 2-methylimidazole, ZIF is zeolitic imidazolate framework; **b–d** TEM images of CoS nanobubble cages; **e** CV curves at a scanning rate of 2.0 $mV \cdot s^{-1}$; **f** rate performance. Reproduced with permission from Ref. [100]. Copyright 2017, Wiley

(Fig. 10b). These self-assembled porous spherical particles show strong affinity for conducting carbon additives, ensuring rapid transfer of electrons and ions to the internal MA nanocrystals. CV measurements are conducted to demonstrate the LICs full cell electrochemical properties at various sweep rates from 5 to 500 $mV \cdot s^{-1}$ (Fig. 10c), and the CV profiles deviate from the quasi-rectangle. These results confirm that the charge storage in the LICs could combine the storage mechanisms between MA@PVDF anode and activated carbon (AC) cathode. In addition, the flexible LICs device is fabricated in the schematic diagram in (Fig. 10d), which delivers 113.6 $Wh \cdot kg^{-1}$ at a high

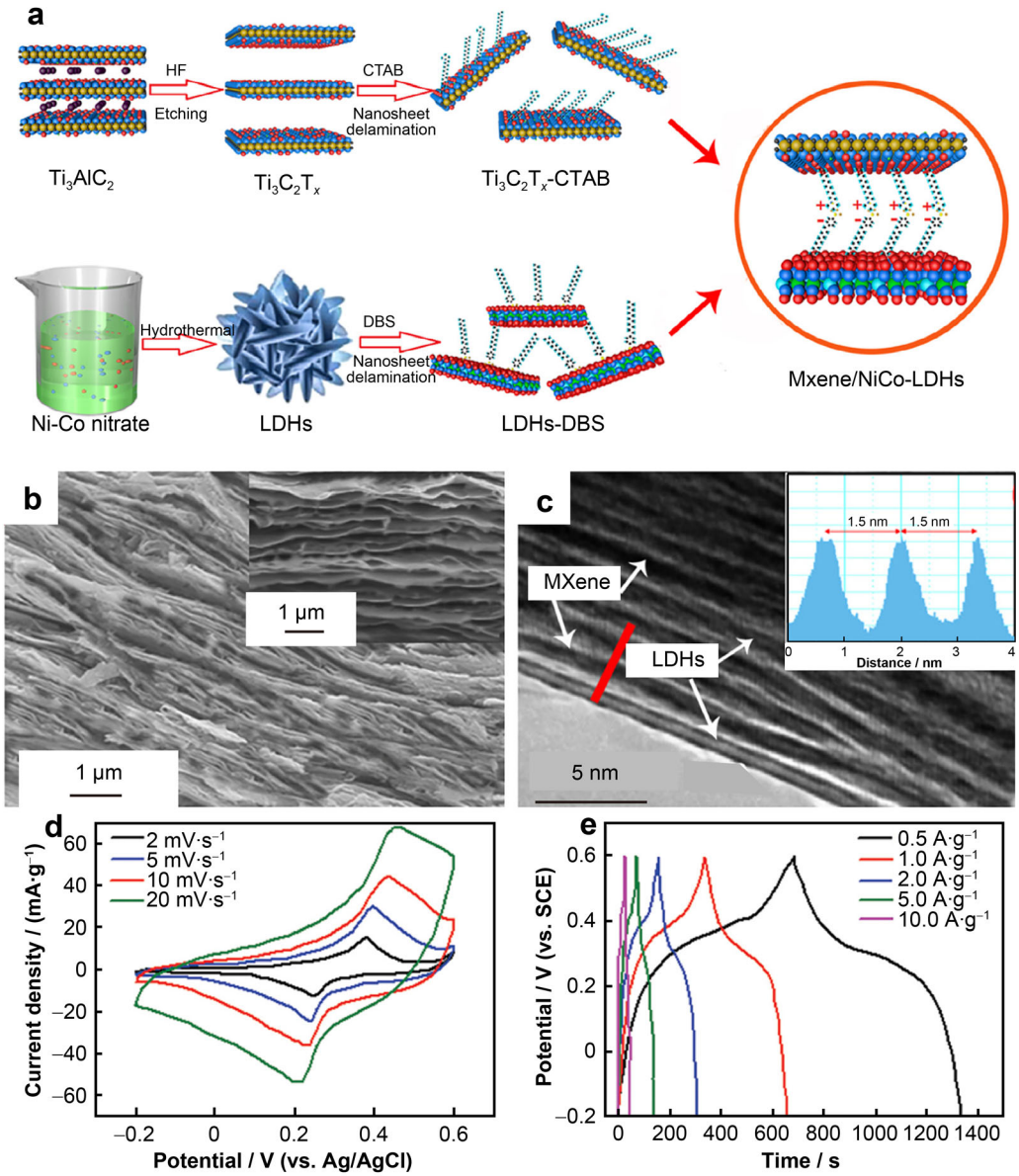

Fig. 9 **a** Schematic illustration for fabrication of 2D MXene/NiCo-LDHs assembly through anions–cations electrostatic adsorption; **b** SEM and **c** TEM images of MXene/NiCo-LDHs and (inset) *d*-spacing of adjacent nanosheets; **d** CV curves of MXene/NiCo-LDHs electrodes at different sweep rates; **e** Galvanostatic charge–discharge curves of MXene/NiCo-LDHs electrode at different current densities. Reproduced with permission from Ref. [107]. Copyright 2020, Elsevier

energy density of 0.1 $A{\cdot}g^{-1}$, with significant cyclic stability in flat and curved states (Fig. 10e). After 30 bending-flatting operations, it could retain 84.5% of the initial energy density. As shown in Fig. 10f, the flexible LICs could deliver energy densities of 153.1, 106.8, 85.2, 52.0 and 22.1 $Wh{\cdot}kg^{-1}$ at the current densities of 0.05, 0.10, 0.20, 0.50 and 1.00 $A{\cdot}g^{-1}$, respectively. These results validate that MA@PVDF has admirable energy density and immense potential for future wearable energy storage applications.

5 Conclusion and prospect

In summary, we have reviewed the recently self-assembly of nanoparticles into highly ordered, multifunctional materials and electrode materials. The mechanism, driving force and research progress of assembly are discussed. In order to improve the structural stability of the assembly, the interaction forces between the assembly units are strengthened from pure particle self-assembly to organic–inorganic co-assembly. The advantage of this assembly

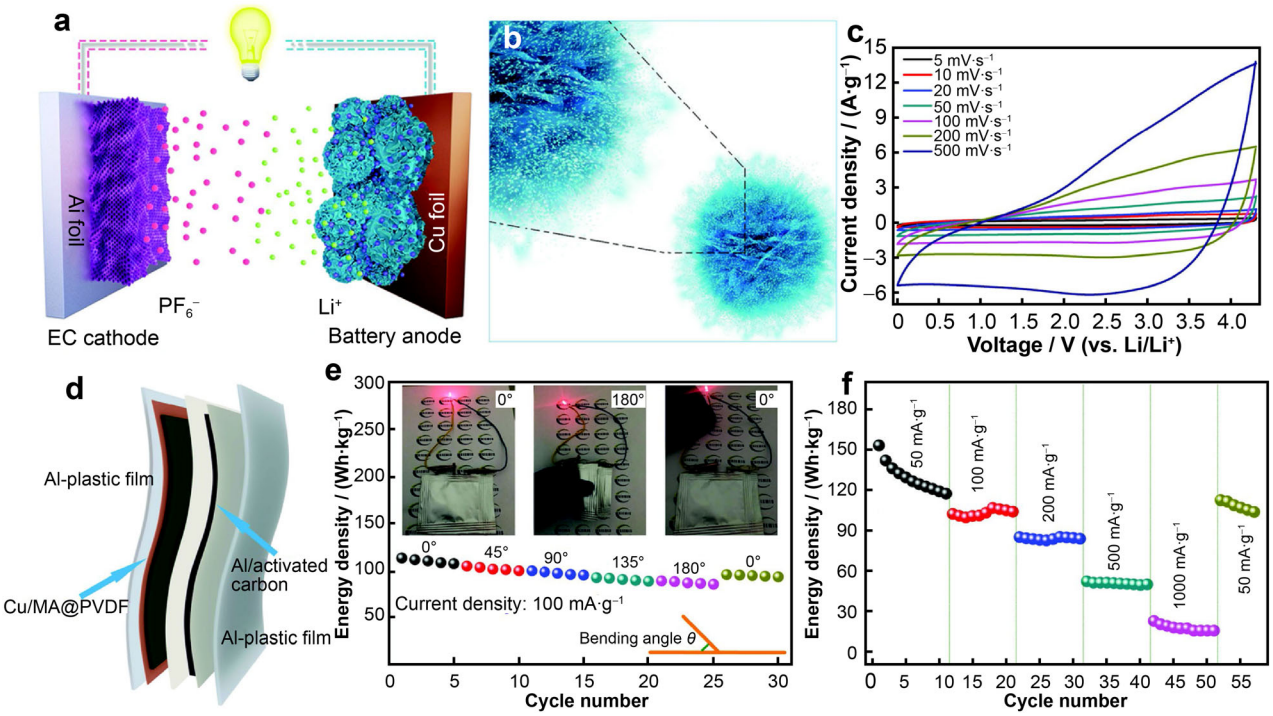

Fig. 10 **a** Schematic illustration of a typical LICs, where EC is electrochemical capacitor; **b** schematic diagram of a single MA@PVDF particle; **c** CV distribution curves of LICs full battery employing MA@PVDF anode and AC cathode at various scanning rates; **d** schematic illustration of flexible MA@PVDF//AC LICs devices; **e** cycling performance of bendable LICs devices at diverse deformation states and (insets) powering red light emitting diode (LED) indicators under different bending conditions; **f** rate performance of flexible LICs devices at different current densities. Reproduced with permission from Ref. [113]. Copyright 2018, Wiley

method is that it collects many single properties into a multi-functional material. These structures had been used in a wide range of industrial catalysis and energy information applications. In addition, there would be unprecedented new performance.

However, there are still many challenges that need to be explored and improved. First of all, the precise control of self-assembly structure and performance is still a great challenge, which requires not only the precise control of the size, nature, and shape of the assembly unit, but also the specific regulation of the assembly conditions. Through the construction of nanoparticle self-assembly, the main research line of "structure-property-performance-application" is finally established. Specifically, in the application of energy storage, compared with a single nanoparticle, the assembly does show good cycling stability. However, due to the weak interaction force between the particles of the assembly, the mechanical properties of the system are poor, so the interaction force between the particles should be further strengthened.

Secondly, the interface self-assembly technology produced a small yield of nanomaterials. At present, nano-self-assembly technology still has bottlenecks in the industrial scaling up of materials. New materials with lower costs should be explored as substitutes for precious metals, semiconductors, and other materials to realize mass industrial production of nano-self-assembly materials. Finally, increasing the complexity of structures by combining other up-bottom and bottom-up approaches is one of the natural directions of nanoscience. It is anticipated that new complex active nanostructures will be synthesized to size by self-assembly assisted by the Pickering emulsion method to explore new properties and applications. Self-assembly is an interdisciplinary subject in the scale of the nanostructure, which requires the joint efforts of researchers from all disciplines to achieve further development.

Acknowledgements This work was financially supported by the National Natural Science Foundation of China (Nos. 51772296, 5217020858, 51902016 and 21975015) and the Fundamental Research Funds for the Central Universities (Nos. buctrc201829 and buctrc201904).

Declarations

Conflict of interests The authors declare that they have no conflict of interest.

References

[1] Grzelczak M, Liz-Marza´n LM, Klajn R. Stimuli-responsive self-assembly of nanoparticles. Chem Soc Rev. 2019;48(5): 1342. https://doi.org/10.1039/C8CS00787J.

[2] Whitesides GM, Grzybowski B. Self-assembly at all scales. Science. 2002;295(5564):2418. https://doi.org/10.1126/science.1070821.

[3] Shi Q, Dong DS, Si KJ, Sikdar D, Yap LW, Premaratne M, Cheng W. Shape transformation of constituent building blocks within self-assembled nanosheets and nano-origami. ACS Nano. 2018;12(2):1014. https://doi.org/10.1021/acsnano.7b08334.

[4] Wang T, LaMontagne D, Lynch J, Zhuang J, Cao YC. Colloidal superparticles from nanoparticle assembly. Chem Soc Rev. 2013;42(7):2804. https://doi.org/10.1039/C2CS35318K.

[5] Jain T, Roodbeen R, Reeler NE, Vosch T, Jensen KJ, Bjornholm T, Norgaard K. End-to-end assembly of gold nanorods via oligopeptide linking and surfactant control. J Colloid Interface Sci. 2012;376:83. https://doi.org/10.1016/j.jcis.2012.03.022.

[6] Dong D, Yap LW, Smilgies DM, Si KJ, Shi Q, Cheng W. Two-dimensional gold trisoctahedron nanoparticle superlattice sheets: self-assembly, characterization and immunosensing applications. Nanoscale. 2018;10(11):5065. https://doi.org/10.1039/C7NR09443D.

[7] Rao SY, Si KJ, Yap LW, Xiang Y, Cheng WL. Free-standing bi-layered nanoparticle superlattice nanosheets with asymmetric ionic transport behaviors. ACS Nano. 2015;9(11): 11218. https://doi.org/10.1021/acsnano.5b04784.

[8] Florea D, Wyss HM. Towards the self-assembly of anisotropic colloids: monodisperse oblate ellipsoids. J Colloid Interface Sci. 2014;416:30. https://doi.org/10.1016/j.jcis.2013.10.027.

[9] Zhao Y, Shang L, Cheng Y, Gu Z. Spherical colloidal photonic crystals. Acc Chem Res. 2014;47(12):3632. https://doi.org/10.1021/ar500317s.

[10] Lucio Isa KK, Mischa Müller JG, Marcus T, Erik R. Particle lithography from colloidal self-assembly at liquid-liquid interfaces. ACS Nano. 2010;4(10):5665. https://doi.org/10.1021/nn101260f.

[11] Ng KC, Udagedara IB, Rukhlenko ID, Chen Y, Tang Y, Premaratne M, Cheng WL. Free-standing plasmonic-nanorod superlattice sheets. ACS Nano. 2012;6(1):925. https://doi.org/10.1021/nn204498j.

[12] Si KJ, Chen Y, Shi Q, Cheng W. Nanoparticle superlattices: the roles of soft ligands. Adv Sci. 2018;5(1):1700179. https://doi.org/10.1002/advs.201700179.

[13] Cui Y, Wei Q, Park H, Lieber CM. Nanowire nanosensors for highly sensitive and selective detection of biological and chemical species. Science. 2001;293(5533):1289. https://doi.org/10.1126/science.1062711.

[14] Duan XF, Huang Y, Cui Y, Wang JF, Lieber CM. Indium phosphide nanowires as building blocks for nanoscale electronic and optoelectronic devices. Nature. 2001;409:66. https://doi.org/10.1038/35051047.

[15] Rymaruk MJ, Cunningham VJ, Brown SL, Williams CN, Armes SP. Oil-in-oil pickering emulsions stabilized by diblock copolymer nanoparticles. J Colloid Interface Sci. 2020;580: 354. https://doi.org/10.1016/j.jcis.2020.07.010.

[16] Liu Q, Sun Z, Santamarina JC. Self-assembled nanoparticle-coated interfaces: capillary pressure, shell formation and buckling. J Colloid Interface Sci. 2021;581:251. https://doi.org/10.1016/j.jcis.2020.07.110.

[17] Lin Z, Zhang Z, Li Y, Deng Y. Magnetic nano-Fe_3O_4 stabilized pickering emulsion liquid membrane for selective extraction and separation. Chem Eng J. 2016;288:305. https://doi.org/10.1016/j.cej.2015.11.109.

[18] Gao Q, Wang C, Liu H, Chen Y, Tong Z. Dual nanocomposite multi-hollow polymer microspheres prepared by suspension polymerization based on a multiple pickering emulsion. Polym Chem. 2010;1:75. https://doi.org/10.1039/B9PY00255C.

[19] Zhou S, Bismarck A, Steinke JHG. Interconnected macroporous glycidyl methacrylate-grafted dextran hydrogels synthesized from hydroxyapatite nanoparticle stabilized high internal phase emulsion templates. J Mater Chem. 2012;22(36):18824. https://doi.org/10.1039/C2JM33294A.

[20] Kempin MV, Stock S, Klitzing R, Kraume M, Drews A. Influence of particle type and concentration on the ultrafiltration behavior of nanoparticle stabilized Pickering emulsions and suspensions. Sep Purif Technol. 2020;252: 117457. https://doi.org/10.1016/j.seppur.2020.117457.

[21] Wang ZG, Li N, Wang T, Ding BQ. Surface-guided chemical processes on self-assembled DNA nanostructures. Langmuir. 2018; 34(49):14954. https://doi.org/10.1021/acs.langmuir.8b01060.

[22] Niehues M, Engel S, Ravoo BJ. Photo-responsive self-assembly of plasmonic magnetic Janus nanoparticles. Langmuir. 2021;37(37):11123. https://doi.org/10.1021/acs.langmuir.1c01979.

[23] Rival JV, Mymoona P, Lakshmi KM, Pradeep T, Hibu ES. Self-assembly of precision noble metal nanoclusters: hierarchical structural complexity, colloidal superstructures, and applications. Small. 2021;17(27):2005718. https://doi.org/10.1002/smll.202005718.

[24] Bao Y, Zhang Y, Liu P, Ma J, Zhang W, Liu C, Simion D. Novel fabrication of stable pickering emulsion and latex by hollow silica nanoparticles. J Colloid Interface Sci. 2019;553: 83. https://doi.org/10.1016/j.jcis.2019.06.008.

[25] Venkataramani D, Tsulaia A, Amin S. Fundamentals and applications of particle stabilized emulsions in cosmetic formulations. Adv Colloid Interface Sci. 2020;283:102234. https://doi.org/10.1016/j.cis.2020.102234.

[26] Aveyard R, Binks BP, Clint JH. Emulsions stabilized solely by colloidal particles. Adv Colloid Interface Sci. 2003;100:503. https://doi.org/10.1016/S0001-8686(02)00069-6.

[27] Binks BP, Murakami R. Phase inversion of particle-stabilized materials from foams to dry water. Nat Mater. 2006;5(11):865. https://doi.org/10.1038/nmat1757.

[28] Binks BP, Lumsdon SO. Influence of particle wettability on the type and stability of surfactant-free emulsions. Langmuir. 2000;16(23):8622. https://doi.org/10.1021/la000189s.

[29] Khedr A, Striolo A. Self-assembly of mono and poly-dispersed nanoparticles on emulsion droplets: antagonistic vs. synergistic effects as a function of particle size. Phys Chem Chem Phys. 2020;22(39):22662. https://doi.org/10.1039/D0CP02588G.

[30] Hils C, Schmelz J, Drechsler M, Schmalz H. Janus micelles by crystallization-driven self-assembly of an amphiphilic, double-crystalline triblock terpolymer. J Am Chem Soc. 2021; 143(38):15582. https://doi.org/10.1021/jacs.1c08076.

[31] Kim BS, Taton TA. Multicomponent nanoparticles via self-assembly with cross-linked block copolymer surfactants. Langmuir. 2007;23:2198. https://doi.org/10.1021/la062692w.

[32] Eck W, Küller A, Grunze M, Völkel B, Gölzhäuser A. Freestanding nanosheets from crosslinked biphenyl self-assembled monolayers. Adv Mater. 2005;17(21):2583. https://doi.org/10.1002/adma.200500900.

[33] Nikoobakht B, El Sayed MA. Evidence for bilayer assembly of cationic surfactants on the surface of gold nanorods. Langmuir. 2001;17:6368. https://doi.org/10.1021/la010530o.

[34] Dinsmore AD, Hsu MF, Nikolaides MG, Marquez M, Bausch AR, Weitz DA. Colloidosomes: selectively permeable capsules

composed of colloidal particles. Science. 2002;298(5595):1006. https://doi.org/10.1126/science.1074868.
[35] Bai F, Wang D, Huo Z, Chen W, Liu L, Liang X, Chen C, Wang X, Peng Q, Li Y. A versatile bottom-up assembly approach to colloidal spheres from nanocrystals. Angew Chem Int Ed. 2007;119(35):6770. https://doi.org/10.1002/ange.200701355.
[36] Liu D, Zhou F, Li C, Zhang T, Zhang H, Cai W, Li Y. Black gold: plasmonic colloidosomes with broadband absorption self-assembled from monodispersed gold nanospheres by using a reverse emulsion system. Angew Chem Int Ed. 2015;54(33):9596. https://doi.org/10.1002/anie.201503384.
[37] Zhao M, Cai B, Ma Y, Cai H, Huang J, Pan X, He H, Ye Z. Self-assemble $ZnMn_2O_4$ hierarchical hollow microspheres into self-supporting architecture for enhanced biosensing performance. Biosens Bioelectron. 2014;61:443. https://doi.org/10.1016/j.bios.2014.05.051.
[38] Lee SH, Yu SH, Lee JE, Jin A, Lee DJ, Lee N, Jo H, Shin K, Ahn TY, Kim YW, Choe H, Sung YE, Hyeon T. Self-assembled Fe_3O_4 nanoparticle clusters as high-performance anodes for lithium-ion batteries via geometric confinement. Nano Lett. 2013;13(9):4249. https://doi.org/10.1021/nl401952h.
[39] Park J, An K, Hwang Y, Park JG, Noh HJ, Kim JY, Park JH, Hwang NM, Hyeon T. Ultra-large-scale syntheses of monodisperse nanocrystals. Nat Mater. 2004;3(12):891. https://doi.org/10.1038/nmat1251.
[40] Buck MR, Biacchi AJ, Schaak RE. Insights into the thermal decomposition of Co(II) oleate for the shape-controlled synthesis of wurtzite-type CoO nanocrystals. Chem Mater. 2014;26(3):1492. https://doi.org/10.1021/cm4041055.
[41] Joo J, Na HB, Yu T, Yu JH, Kim YW, Wu F, Zhang JZ, Hyeon T. Generalized and facile synthesis of semiconducting metal sulfide nanocrystals. J Am Chem Soc. 2003;125(36):11100. https://doi.org/10.1021/ja0357902.
[42] Walther A, Muller AHE. Janus particles: synthesis, self-assembly, physical properties, and applications. Chem Rev. 2013;113(7):5194. https://doi.org/10.1021/cr300089t.
[43] Chen D, Amstad E, Zhao CX, Cai L, Fan J, Chen Q, Hai M, Koehler S, Zhang H, Liang F, Yang Z, Weitz DA. Biocompatible amphiphilic hydrogel-solid dimer particles as colloidal surfactants. ACS Nano. 2017;11(12):11978. https://doi.org/10.1021/acsnano.7b03110.
[44] Liu Y, Deng K, Yang J, Wu X, Fan X, Tang M, Quan Z. Shape-directed self-assembly of nano dumbbells into superstructure polymorphs. Chem Sci. 2020;11(16):4065. https://doi.org/10.1039/D0SC00592D.
[45] Lu Y, Lin J, Wang L, Zhang L, Cai C. Self-assembly of copolymer micelles: higher-level assembly for constructing hierarchical structure. Chem Rev. 2020;120(9):4111. https://doi.org/10.1021/acs.chemrev.9b00774.
[46] Tang Z, Gao L, Lin J, Cai C, Yao Y, Guerin G, Tian X, Lin S. Anchorage-dependent living supramolecular self-assembly of polymeric micelles. J Am Chem Soc. 2021;143(36):14684. https://doi.org/10.1021/jacs.1c06020.
[47] Karayianni M, Pispas S. Block copolymer solution self-assembly: recent advances, emerging trends, and applications. J Polym Sci. 2021;59(17):1874. https://doi.org/10.1002/pol.20210430.
[48] Zhu J, Hayward RC. Hierarchically structured microparticles formed by interfacial instabilities of emulsion droplets containing amphiphilic block copolymers. Angew Chem Int Ed. 2008;47(11):2113. https://doi.org/10.1002/ange.200704863.
[49] Tagliabue A, Izzo L, Mella M. Out of equilibrium self-assembly of Janus nanoparticles: steering it from disordered amorphous to 2D patterned aggregates. Langmuir. 2016;32(48):12934. https://doi.org/10.1021/acs.langmuir.6b02715.
[50] Gai Y, Lin Y, Song DP, Yavitt BM, Watkins JJ. Strong ligand-block copolymer interactions for incorporation of relatively large nanoparticles in ordered composites. Macromolecules. 2016;49(9):3352. https://doi.org/10.1021/acs.macromol.5b02609.
[51] Ha JM, Lim SH, Dey J, Lee SJ, Lee MJ, Kang SH, Jin KS, Choi SM. Micelle-assisted formation of nanoparticle superlattices and thermally reversible symmetry transitions. Nano Lett. 2019;19(4):2313. https://doi.org/10.1021/acs.nanolett.8b04817.
[52] Zubarev ER, Xu J, Sayyad A, Gibson JD. Amphiphilicity-driven organization of nanoparticles into discrete assemblies. J Am Chem Soc. 2006;128(47):15098. https://doi.org/10.1021/ja066708g.
[53] Guo Y, Saei SH, Izumi CMS, Moffitt MG. Block copolymer mimetic self-assembly of inorganic nanoparticles. ACS Nano. 2011;5(4):3309. https://doi.org/10.1021/nn200450c.
[54] Li X, Li H, Liu G, Deng Z, Wu S, Li P, Xu Z, Xu H, Chu PK. Magnetite-loaded fluorine-containing polymeric micelles for magnetic resonance imaging and drug delivery. Biomaterials. 2012;33(10):3013. https://doi.org/10.1016/j.biomaterials.2011.12.042.
[55] Cao W, Xia S, Jiang X, Appold M, Opel M, Plank M, Schaffrinna R, Kreuzer LP, Yin S, Gallei M, Schwartzkopf M, Roth SV, Muller Buschbaum P. Self-assembly of large magnetic nanoparticles in ultrahigh molecular weight linear diblock copolymer films. ACS Appl Mater Interfaces. 2020;12(6):7557. https://doi.org/10.1021/acsami.9b20905.
[56] Kao J, Xu T. Nanoparticle assemblies in supramolecular nanocomposite thin films: concentration dependence. J Am Chem Soc. 2015;137(19):6356. https://doi.org/10.1021/jacs.5b02494.
[57] Yuan Q, Russell TP, Wang D. Self-assembly behavior of PS-b-P2VP block copolymers and carbon quantum dots at water/oil interfaces. Macromolecules. 2020;53(24):10981. https://doi.org/10.1021/acs.macromol.0c02422.
[58] Wang M, Zhang M, Siegers C, Scholes GD, Winnik MA. Polymer vesicles as robust scaffolds for the directed assembly of highly crystalline nanocrystals. Langmuir. 2009;25(24):13703. https://doi.org/10.1021/la900523s.
[59] Hickey RJ, Meng X, Zhang P, Park SJ. Low-dimensional nanoparticle clustering in polymer micelles and their transverse relaxivity rates. ACS Nano. 2013;7(7):5824. https://doi.org/10.1021/nn400824b.
[60] Li W, Liu S, Deng R, Zhu J. Encapsulation of nanoparticles in block copolymer micellar aggregates by directed supramolecular assembly. Angew Chem Int Ed. 2011;50(26):5865. https://doi.org/10.1002/anie.201008224.
[61] Choueiri RM, Klinkova A, Therien Aubin H, Rubinstein M, Kumacheva E. Structural transitions in nanoparticle assemblies governed by competing nanoscale forces. J Am Chem Soc. 2013;135(28):10262. https://doi.org/10.1021/ja404341r.
[62] Sanwaria S, Horechyy A, Wolf D, Chu CY, Chen HL, Formanek P, Stamm M, Srivastava R, Nandan B. Helical packing of nanoparticles confined in cylindrical domains of a self-assembled block copolymer structure. Angew Chem Int Ed. 2014;53(34):9090. https://doi.org/10.1002/anie.201403565.
[63] Singh S, Samanta P, Srivastava R, Horechyy A, Reuter U, Stamm M, Chen HL, Nandan B. Ligand displacement induced morphologies in block copolymer/quantum dot hybrids and formation of core-shell hybrid nanoobjects. Phys Chem Chem Phys. 2017;19(40):27651. https://doi.org/10.1039/C7CP04343K.
[64] Jang SG, Khan A, Hawker CJ, Kramer EJ. Morphology evolution of PS-b-P2VP diblock copolymers via supramolecular assembly of hydroxylated gold nanoparticles. Macromolecules. 2012;45(3):1553. https://doi.org/10.1021/ma202391k.

[65] Lin Y, Daga VK, Anderson ER, Gido SP, Watkins JJ. Nanoparticle-driven assembly of block copolymers: a simple route to ordered hybrid materials. J Am Chem Soc. 2011; 133(17):6513. https://doi.org/10.1021/ja2003632.
[66] Krack M, Hohenberg H, Kornowski A, Lindner P, Weller H, Förster S. Nanoparticle-loaded magnetophoretic vesicles. J Am Chem Soc. 2008;130(23):7315. https://doi.org/10.1021/ja077398k.
[67] Deng R, Li H, Zhu J, Li B, Liang F, Jia F, Qu X, Yang Z. Janus nanoparticles of block copolymers by emulsion solvent evaporation induced assembly. Macromolecules. 2016;49(4):1362. https://doi.org/10.1021/acs.macromol.5b02507.
[68] Yang Z, Altantzis T, Zanaga D, Bals S, Tendeloo GV, Pileni MP. Supracrystalline colloidal eggs: epitaxial growth and freestanding three-dimensional supracrystals in nanoscaled colloidosomes. J Am Chem Soc. 2016;138(10):3493. https://doi.org/10.1021/jacs.5b13235.
[69] Sanchez Iglesias A, Grzelczak M, Altantzis T, Goris B, Perez Juste J, Bals S, Van Tendeloo G, Donaldson SH Jr, Chmelka BF, Israelachvili JN, Liz Marzan LM. Hydrophobic interactions modulate self-assembly of nanoparticles. ACS Nano. 2012;6(12):11059. https://doi.org/10.1021/nn3047605.
[70] Zhu J, Hayward RC. Spontaneous generation of amphiphilic block copolymer micelles with multiple morphologies through interfacial instabilities. J Am Chem Soc. 2008;130(23):7496. https://doi.org/10.1021/ja801268e.
[71] Ren M, Hou Z, Zheng X, Xu J, Zhu J. Electrostatic control of the three-dimensional confined assembly of charged block copolymers in emulsion droplets. Macromolecules. 2021; 54(12):5728. https://doi.org/10.1021/acs.macromol.1c00575.
[72] Yan N, Liu X, Zhu J, Zhu Y, Jiang W. Well-ordered inorganic nanoparticle arrays directed by block copolymer nanosheets. ACS Nano. 2019;13(6):6638. https://doi.org/10.1021/acsnano.9b00940.
[73] Sánchez-Iglesias A, Claes N, Solis DM, Taboada JM, Bals S, Liz Marzan LM, Grzelczak M. Reversible clustering of gold nanoparticles under confinement. Angew Chem Int Ed. 2018; 57(12):3183. https://doi.org/10.1002/ange.201800736.
[74] Luo QJ, Hickey RJ, Park SJ. Controlling the location of nanoparticles in colloidal assemblies of amphiphilic polymers by tuning nanoparticle surface chemistry. ACS Macro Lett. 2013;2(2):107. https://doi.org/10.1021/mz3006044.
[75] Li W, Zhang P, Dai M, He J, Babu T, Xu YL, Deng R, Liang R, Lu MH, Nie Z, Zhu J. Ordering of gold nanorods in confined spaces by directed assembly. Macromolecules. 2013;46(6): 2241. https://doi.org/10.1021/ma400115z.
[76] He L, Zhang L, Liang H. Mono- or bidisperse nanorods mixtures in diblock copolymers. Polymer. 2010;51(14):3303. https://doi.org/10.1016/j.polymer.2010.05.026.
[77] El-Kady MF, Strong V, Dubin S, Kaner RB. Laser scribing of high-performance and flexible graphene-based electrochemical capacitors. Science. 2012;335(6074):1326. https://doi.org/10.1126/science.1216744.
[78] Jiang SH, Ding J, Wang RH, Chen FY, Sun J, Deng YX, Li XL. Solvothermal-induced construction of ultra-tiny Fe_2O_3 nanoparticles/graphene hydrogels as binder-free high-capacitance anode for supercapacitors. Rare Met. 2021;40(12):3520. https://doi.org/10.1007/s12598-021-01739-8.
[79] Simon P, Gogotsi Y. Materials for electrochemical capacitors. Nat Mater. 2008;7:845. https://doi.org/10.1142/9789814287005_0033.
[80] Shen L, Yu L, Wu HB, Yu XY, Zhang X, Lou XW. Formation of nickel cobalt sulfide ball-in-ball hollow spheres with enhanced electrochemical pseudocapacitive properties. Nat Commun. 2015;6:6694. https://doi.org/10.1038/ncomms7694.
[81] Yu L, Guan BY, Xiao W, Lou XW. Formation of yolk-shelled Ni-Co mixed oxide nanoprisms with enhanced electrochemical performance for hybrid supercapacitors and lithium-ion batteries. Adv Energy Mater. 2015;5(21):1500981. https://doi.org/10.1002/aenm.201500981.
[82] Ren Y, Hardwick LJ, Bruce PG. Lithium intercalation into mesoporous anatase with an ordered 3D pore structure. Angew Chem Int Ed. 2010;122(14):2624. https://doi.org/10.1002/ange.200907099.
[83] Ji HX, Zhao X, Qiao ZH, Jung J, Zhu YW, Lu YL, Zhang LL, MacDonald AH, Ruoff RS. Capacitance of carbon-based electrical double-layer capacitors. Nat Commun. 2014;5:3317. https://doi.org/10.1038/ncomms4317.
[84] Wang FX, Wu XW, Yuan XH, Liu ZC, Zhang Y, Fu LJ, Zhu YS, Zhou QM, Wu YP, Huang W. Latest advances in supercapacitors: from new electrode materials to novel device designs. Chem Soc Rev. 2017;46:6816. https://doi.org/10.1039/C7CS00205J.
[85] Chmiola J, Largeot C, Taberna PL, Simon P, Gogotsi Y. Monolithic carbide-derived carbon films for micro-supercapacitors. Science. 2010;328(5977):480. https://doi.org/10.1126/science.1184126.
[86] Li H, Zhu Y, Dong S, Shen L, Chen Z, Zhang X, Yu G. Self-assembled Nb_2O_5 nanosheets for high energy-high power sodium ion capacitors. Chem Mater. 2016;28(16):5753. https://doi.org/10.1021/acs.chemmater.6b01988.
[87] Huang J, Xiao YB, Peng ZY, Xu YZ, Li LB, Tan LC, Yuan K, Chen YW. Co_3O_4 supraparticle-based bubble nanofiber and bubble nanosheet with remarkable electrochemical performance. Adv Sci. 2019;6(12):1900107. https://doi.org/10.1002/advs.201900107.
[88] Zhang JT, Hu H, Li Z, Lou XW. Double-shelled nanocages with cobalt hydroxide inner shell and layered double hydroxides outer shell as high-efficiency polysulfide mediator for lithium-sulfur batteries. Angew Chem Int Ed. 2016;128(12): 4050. https://doi.org/10.1002/ange.201511632.
[89] Xia BY, Yan Y, Li N, Wu HB, Lou XW, Wang X. A metal-organic framework-derived bifunctional oxygen electrocatalyst. Nat Energy. 2016;1:15006. https://doi.org/10.1038/nenergy.2015.6.
[90] Hu H, Han L, Yu MZ, Wang ZY, Lou XW. Metal-organic-framework-engaged formation of Co nanoparticle-embedded carbon@Co_9S_8 double-shelled nanocages for efficient oxygen reduction. Energy Environ Sci. 2016;9:107. https://doi.org/10.1039/C5EE02903A.
[91] Cai XJ, Gao W, Ma M, Wu MY, Zhang LL, Zheng YY, Chen HR, Shi JL. A Prussian blue-based core-shell hollow-structured mesoporous nanoparticle as a smart theranostic agent with ultrahigh pH-responsive longitudinal relaxivity. Adv Mater. 2015;27(41):6382. https://doi.org/10.1002/adma.201503381.
[92] Hu L, Chen QW. Hollow/porous nanostructures derived from nanoscale metal-organic frameworks towards high performance anodes for lithium-ion batteries. Nanoscale. 2014;6(3): 1236. https://doi.org/10.1039/C3NR05192G.
[93] Zhang L, Wu HB, Lou XW. Metal-organic-frameworks-derived general formation of hollow structures with high complexity. J Am Chem Soc. 2013;135(29):10664. https://doi.org/10.1021/ja401727n.
[94] Liu J, Wu C, Xiao DD, Kopold P, Gu L, van Aken PA, Maier J, Yu Y. MOF-derived hollow Co_9S_8 nanoparticles embedded in graphitic carbon nanocages with superior Li-ion storage. Small. 2016;12(17):2354. https://doi.org/10.1002/smll.201503821.
[95] Wu RB, Wang DP, Rui XH, Liu B, Zhou K, Law AWK, Yan QY, Wei J, Chen Z. In-situ formation of hollow hybrids composed of cobalt sulfides embedded within porous carbon polyhedra/carbon nanotubes for high-performance lithium-ion

batteries. Adv Mater. 2015;27(19):3038. https://doi.org/10.1002/adma.201500783.
[96] Chen YM, Yu L, Lou XW. Hierarchical tubular structures composed of Co_3O_4 hollow nanoparticles and carbon nanotubes for lithium storage. Angew Chem Int Ed. 2016;55(20):5990–3. https://doi.org/10.1002/anie.201600133.
[97] Han L, Yu XY, Lou XW. Formation of Prussian-blue-analog nanocages via a direct etching method and their conversion into Ni-Co-mixed oxide for enhanced oxygen evolution. Adv Mater. 2016;28(23):4601. https://doi.org/10.1002/adma.201506315.
[98] Zou F, Hu XL, Li Z, Qie L, Hu CC, Zeng R, Jiang Y, Huang YH. MOF-derived porous ZnO/$ZnFe_2O_4$/C octahedra with hollow interiors for high-rate lithium-ion batteries. Adv Mater. 2014;26(38):6622–8. https://doi.org/10.1002/adma.201402322.
[99] Yu L, Yang JF, Lou XW. Formation of CoS_2 nanobubble hollow prisms for highly reversible lithium storage. Angew Chem Int Ed. 2016;128(43):13620. https://doi.org/10.1002/ange.201606776.
[100] Guan BY, Lou XW. Complex cobalt sulfide nanobubble cages with enhanced electrochemical properties. Small Methods. 2017;1(7):1700158. https://doi.org/10.1002/smtd.201700158.
[101] Zhao R, Wang M, Zhao D, Li H, Wang C, Yin L. Molecular-level heterostructures assembled from titanium carbide MXene and Ni-Co-Al layered double hydroxide nanosheets for All-solid-state flexible asymmetric high-energy supercapacitors. ACS Energy Lett. 2018;3(1):132. https://doi.org/10.1021/acsenergylett.7b01063.
[102] Xie XQ, Zhao MQ, Anasori B, Maleski K, Ren CE, Li J, Byles BW, Pomerantseva E, Wang GX, Gogotsi Y. Porous heterostructured MXene/carbon nanotube composite paper with high volumetric capacity for sodium-based energy storage devices. Nano Energy. 2016;26:513. https://doi.org/10.1016/j.nanoen.2016.06.005.
[103] Zhao RZ, Qian Z, Liu ZY, Zhao DY, Hui XB, Jiang GZ, Wang CX, Yin LW. Molecular-level heterostructures assembled from layered black phosphorene and Ti_3C_2 MXene as superior anodes for high-performance sodium ion batteries. Nano Energy. 2019;65:104037. https://doi.org/10.1016/j.nanoen.2019.104037.
[104] Zhao RZ, Di HX, Hui XB, Zhao DY, Wang RT, Wang CX, Yin LW. Self-assembled Ti_3C_2 MXene and N-rich porous carbon hybrids as superior anodes for high-performance potassium-ion batteries. Energy Environ Sci. 2020;13:246. https://doi.org/10.1039/D1EE90043A.
[105] Ling Z, Ren CE, Zhao MQ, Yang J, Giammarco JM, Qiu J, Barsoum MW, Gogotsi Y. Flexible and conductive MXene films and nanocomposites with high capacitance. Proc Natl Acad Sci USA. 2014;111:16676. https://doi.org/10.1073/pnas.1414215111.
[106] Hui XB, Ge XL, Zhao RZ, Li ZQ, Yin LW. Interface chemistry on MXene-based materials for enhanced energy storage and conversion performance. Adv Funct Mater. 2020;30(50):2005190. https://doi.org/10.1002/adfm.202005190.
[107] Wu XM, Huang B, Wang QG, Wang Y. High energy density of two-dimensional MXene/NiCo-LDHs interstratification assembly electrode: understanding the role of interlayer ions and hydration. Chem Eng J. 2020;380:122456. https://doi.org/10.1016/j.cej.2019.122456.
[108] Ding J, Hu WB, Paek ES, Mitlin D. Review of hybrid ion capacitors: from aqueous to lithium to sodium. Chem Rev. 2018;118:6457. https://doi.org/10.1021/acs.chemrev.8b00116.
[109] Wang HW, Zhu CR, Chao DL, Yan QY, Fan HJ. Nonaqueous hybrid lithium-ion and sodium-ion capacitors. Adv Mater. 2017;29(46):1702093. https://doi.org/10.1002/adma.201702093.
[110] Kang R, Zhu WQ, Li S, Zou BB, Wang LL, Li GC, Liu XH, Ng DHL, Qiu JX, Zhao Y, Qiao F, Lian JB. Fe_2TiO_5 nanochains as anode for high-performance lithium-ion capacitor. Rare Met. 2021;40(9):2424. https://doi.org/10.1007/s12598-020-01638-4.
[111] Liu JL, Wang J, Xu CH, Jiang H, Li CZ, Zhang LL, Lin JY, Shen ZX. Advanced energy storage devices: basic principles, analytical methods, and rational materials design. Adv Sci. 2018;5(1):1700322. https://doi.org/10.1002/advs.201700322.
[112] Wang YG, Song YF, Xia YY. Electrochemical capacitors: mechanism, materials, systems, characterization and applications. Chem Soc Rev. 2016;45:5925. https://doi.org/10.1039/C5CS00580A.
[113] Hu ZL, Sayed S, Jiang T, Zhu XY, Lu C, Wang GL, Sun JY, Rashid A, Yan CL, Zhang L, Liu ZF. Self-assembled binary organic granules with multiple lithium uptake mechanisms toward high-energy flexible lithium-ion hybrid supercapacitors. Adv Energy Mater. 2018;8(30):1802273. https://doi.org/10.1002/aenm.201802273.

Nian-Wu Li received his Ph.D. degree from Nanjing University of Aeronautics and Astronautics in 2014. After graduation, he worked at the Institute of Chemistry, Chinese Academy of Sciences (ICCAS) as a Postdoctoral Fellow and then joined Beijing Institute of Nano-energy and Nano-systems as an Assistant Professor in 2017. Currently, he is an Associate Professor in Beijing University of Chemical Technology. His research interests focus on advanced materials for energy storage devices (lithium secondary batteries, sodium secondary batteries, solid-state batteries).

Le Yu received his B. Eng. degree in Material Engineering from Shandong University in 2008, M.S. degree in chemistry from Shanghai University in 2011, and Ph.D. degree in Chemical Engineering from Nanyang Technological University in 2016. He is currently a Full Professor at Beijing University of Chemical Technology. His research interests include nanostructured materials for post LIBs, HSCs, and electrocatalysis.

Bao Wang received his Ph.D. degree in Physical Chemistry in 2011 from the Institute of Chemistry Chinese Academy of Sciences. He worked at Nanyang Technological University as a Postdoctoral Research Fellow (2011–2013), Oregon State University as a Postdoctoral Scholar (2013–2014), and Seoul National University as a Senior Researcher (2014–2015), respectively. In 2016, he joined Institute of Process Engineering Chinese Academy of Sciences (IPE CAS) and took a professor position. Prof. Wang's research interests are focused on fabrication of and application of nanostructured inorganic materials in the field of energy and biomedicine.